New Mexico Bureau of Mines and Mineral Resources

Open-File Report 133

A TWO-DIMENSIONAL HYDROLOGIC MODEL OF THE ANIMAS VALLEY, HIDALGO COUNTY, NEW MEXICO

Keith M. O'Brien
Hydrologist

and

William J. Stone
Hydrogeologist

January 1983

TABLE OF CONTENTS

INTRODUCTION

The Animas Valley

The Animas Valley is a topographically closed basin located in western Hidalgo County, southwest New Mexico (fig. 1). The valley is approximately 80 mi long, lying roughly between the Mexican border and US highway 70. The width of the valley varies from 6 to 12 mi along its length. The area of the surface-water drainage basin is 2,341 sq mi.

The Animas Valley lies in the Mexican Highlands section of the Basin and Range physiographic province. It is bounded on the west by the Peloncillo Mountains and on the east by the Pyramid Mountains, and the Animas Mountains (fig. 1). These mountains rise 1,000 to 2,000 ft (300 to 600 m) above the valley floor. The northern topographic boundary is marked by an extensive eolian dune field just south of US 70. The southern topographic divide lies six miles across the international boundary in Mexico.

The climate of the Animas Valley is arid to semi-arid (Cox, 1973). Precipitation generally averages 10 inches (250 mm) in the valley and 22 inches (560 mm) in the higher mountains. Based on 30 years of data (1931-1960), precipitation at Lordsburg falls below 5.71 inches (145 mm) and exceeds 13.84 inches (352 mm) one year in ten. Rainfall is greatest in late summer and early fall; half of the average annual precipitation occurs in July through September. Animas Creek, which rises in the southern Peloncillo Mountains and flows northerly to a point just south of the town of Animas, is the only perennial stream in the study area. Ephemeral surface-water flow occurs along alluvial fans that are

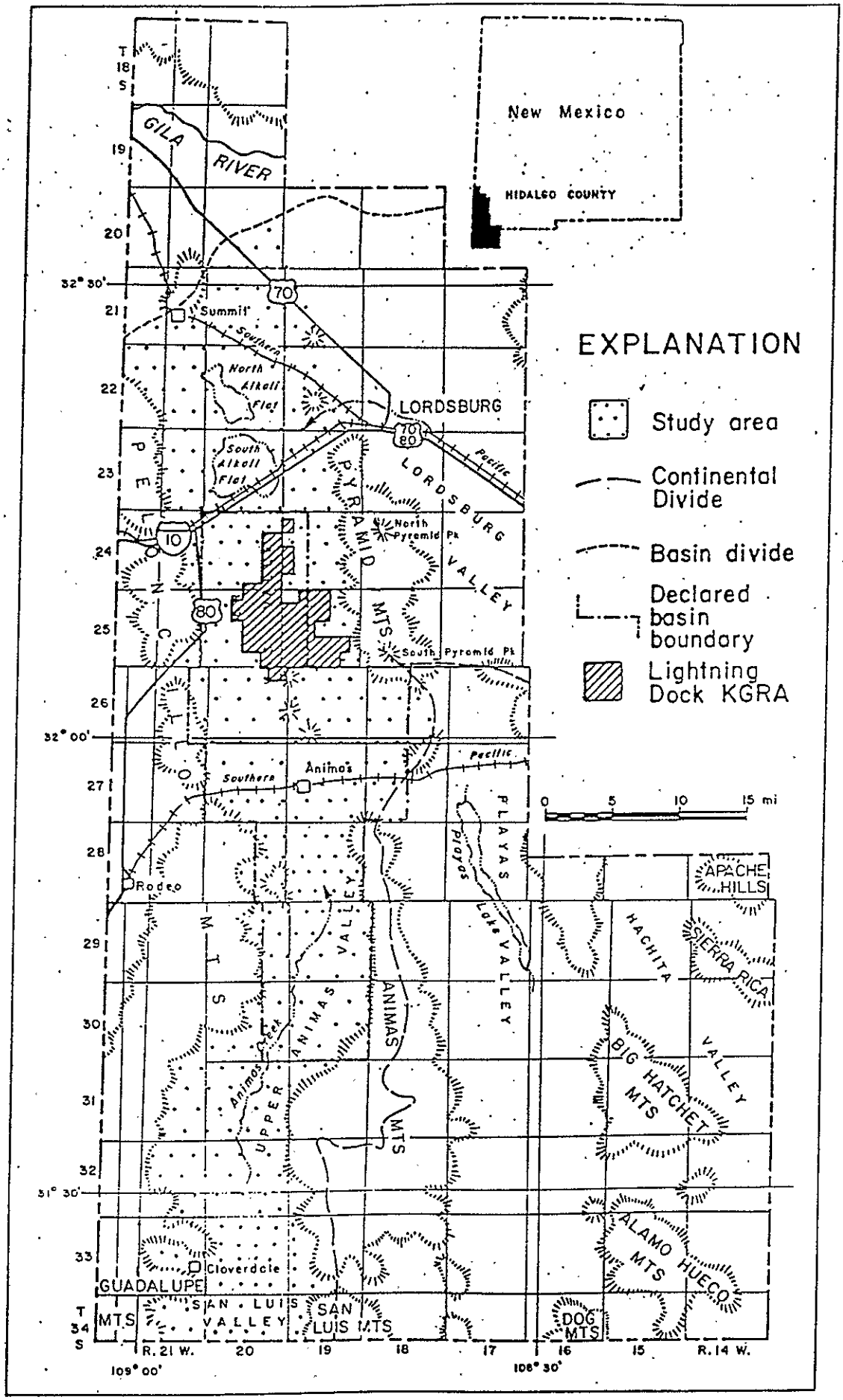

Figure 1 Location of Study Area

located along the west and east valley margins.

Problem and purpose of study

The central part of the valley is an important area for irrigated agriculture (Lansford et al., 1980) and is the site of the Lightning Dock Known Geothermal Resource Area (fig. 1). Although an understanding of the hydrogeology of the valley is important to both the agricultural economy and the development of the area's geothermal resources, the water resources of the entire area have not been studied in detail since 1957 (Reeder, 1957). The Animas Valley is also an excellent example of a closed alluvial basin. For these reasons the present study was initiated as part of the U.S. Geological Survey Water-Resource Division's Southwest Alluvial Basin Regional Aquifer System Analysis. Research supported by the U.S. Geological Survey, Department of Interior under USGS Agreement No. 14-08-0001-18812.

Purpose of this report

Basic data compiled for the Animas Valley study have been released in a series of New Mexico Bureau of Mines and Mineral Resources Open-file reports so that the information compiled would be available for use prior to the completion of the project. O'Brien and Stone (1981) gave the basic water-level data, O'Brien and Stone (1982a) gave the basic water-quality data, and O'Brien and Stone (1982b) gave the drill-hole and testing data. This report is the final project report and gives the two-dimensional hydrologic model developed for the Animas Valley.

Previous Work

Previous geological investigations in the Animas Valley include works by Lasky (1938), Gillerman (1958), Flege (1959), Wrucke and Bromfield (1961), Zeller (1962), Soulè (1972), Thorman and Drewes (1978), Armstrong, et al. (1978), Deal, et al. (1978), Elston, et al. (1979), Drewes and Thorman (198Ø, 198Øa), Lepley (1981), Lohse (1981), Hayes (1982), Fleischhauer and Stone (1982), and Drewes (1982).

Previous geophysical work in the Animas Valley includes investigations by Jiracek and Smith (1976), Smith (1978), Wynn (1981), Lance, et al. (1982), and Ackermann (written communication, 1982).

Previous hydrogeological studies in the Animas Valley were conducted by Schwennesen (1918), Reeder (1957), Arras (1979), Logsdon (1981), Hawkins (1981), and Hawkins and Stephens (1981). Schwennesen (1918) examined the surficial deposits and occurrence of ground water in the Animas, Playas, Hachita, and San Luis basins. Reeder (1957) collected hydrologic data from 1948 to 1955 in order to evaluate the effects of pumping on the ground-water supply of the Animas Valley. Arras (1979) investigated the aquifer characteristics of the Lightning Dock Known Geothermal Resource Area (KGRA) located on the eastern margin of the Animas Valley. Logsdon (1981) conducted a detailed geochemical study of the Lightning Dock KGRA. Hawkins (1981) investigated the ground-water flow system in and adjacent to the Lightning Dock KGRA through the use of a two-dimensional computer model. Hawkins and Stephens (1981) updated the hydrogeothermal data base in the Lightning Dock KGRA and presented the previous research by

Hawkins (1981).

Acknowledgments

The authors wish to acknowledge the assistance of Allan Sanford and John Schlue (Geoscience Department, New Mexico Tech) with interpretation of geophysical data. Special thanks are due Daniel Stephens (Geoscience Department, New Mexico Tech) and David Hawkins (Hargis and Montgomery, Inc.) for invaluable discussions of their research on the Animas Valley, as well as comments on our work.

GEOLOGIC SETTING

Geologic History

Two major tectonic events are evident in the Animas Valley. The present physiography is an expression of the most recent tectonic event. According to Drewes (1982), the main phase of the Laramide orogeny occurred around 75 m.y. ago. It is associated with compressional deformation producing extensive thrust plates originating along northwest trending basement faults. Thrusting was followed by widespread magmatism.

After the Laramide orogeny, tensional conditions replaced compression. The region was topographically high during the Eocene and was deeply eroded with the detritus transported out of the region.

The Basin and Range tectonic event of middle to late Tertiary age reflects an east-west oriented tensional stress system resulting in block-faulting, renewed volcanism, emplacement of granitic plutons, and formation of cauldron complexes. High-angle normal faulting associated with block faulting occurred during the latest stage of the tectonic event. The basin was occupied by Lake Animas in Late Pleistocene and Holocene times (Fleischhauer and Stone, 1982). The period since the Pleistocene has been characterized by some faulting and erosion. Intermontane basins that formed during the latest stage of Basin and Range tectonism have continued to receive sediments since the mid-Miocene.

Surface Geology

The rocks exposed in the bordering mountain ranges consist of Precambrian granodiorite, Paleozoic and Mesozoic sedimentary rocks, Tertiary/Cretaceous volcanic rocks, Tertiary intrusive rocks, Tertiary conglomerate, Quaternary/Tertiary basalt flows, and Quaternary/Tertiary conglomerate (fig. 2). Tertiary intrusive rocks include a 34.9 m.y. old stock in the Animas Mountains, a 30-33 m.y. old quartz-monzonite-porphyry stock in the Peloncillo Mountains, and a 56 m.y. old granodiorite stock in the northern Pyramid Mountains. Tertiary volcanic rocks have been dated in the Peloncillo Mountains near Road Forks at 41.7 m.y. and in the northern Pyramid Mountains southwest of Lordsburg at 67 m.y. The Pyramid Mountains are chiefly composed of Oligocene rhyolitic to andesitic rocks. Two Quaternary/Tertiary basalt flows west of the town of Animas have been dated at 4.4 m.y. and 0.14 m.y. The northwest-southeast trending exposure of Precambrian, Paleozoic, and Mesozoic rocks corresponds roughly to the thrust zone shown on figure 3 and the northwest-southeast trend of gravity highs shown on figure 4.

Elston et al. (1979) delineated approximate limits of cauldron-outer-ring-fracture zones associated with Tertiary volcanics in Hidalgo County (fig. 3). Delineation of the major faults in figure 3 is based on geologic field mapping, Landsat imagery, complete and residual Bouguer gravity anomalies, and seismic refraction profiles.

Fleischhauer and Stone (1982) identified and dated three shorelines of Pleistocene/Holocene Lake Animas. At its highest stage, Lake Animas in Pleistocene time was 17 mi (27 km) long, 8

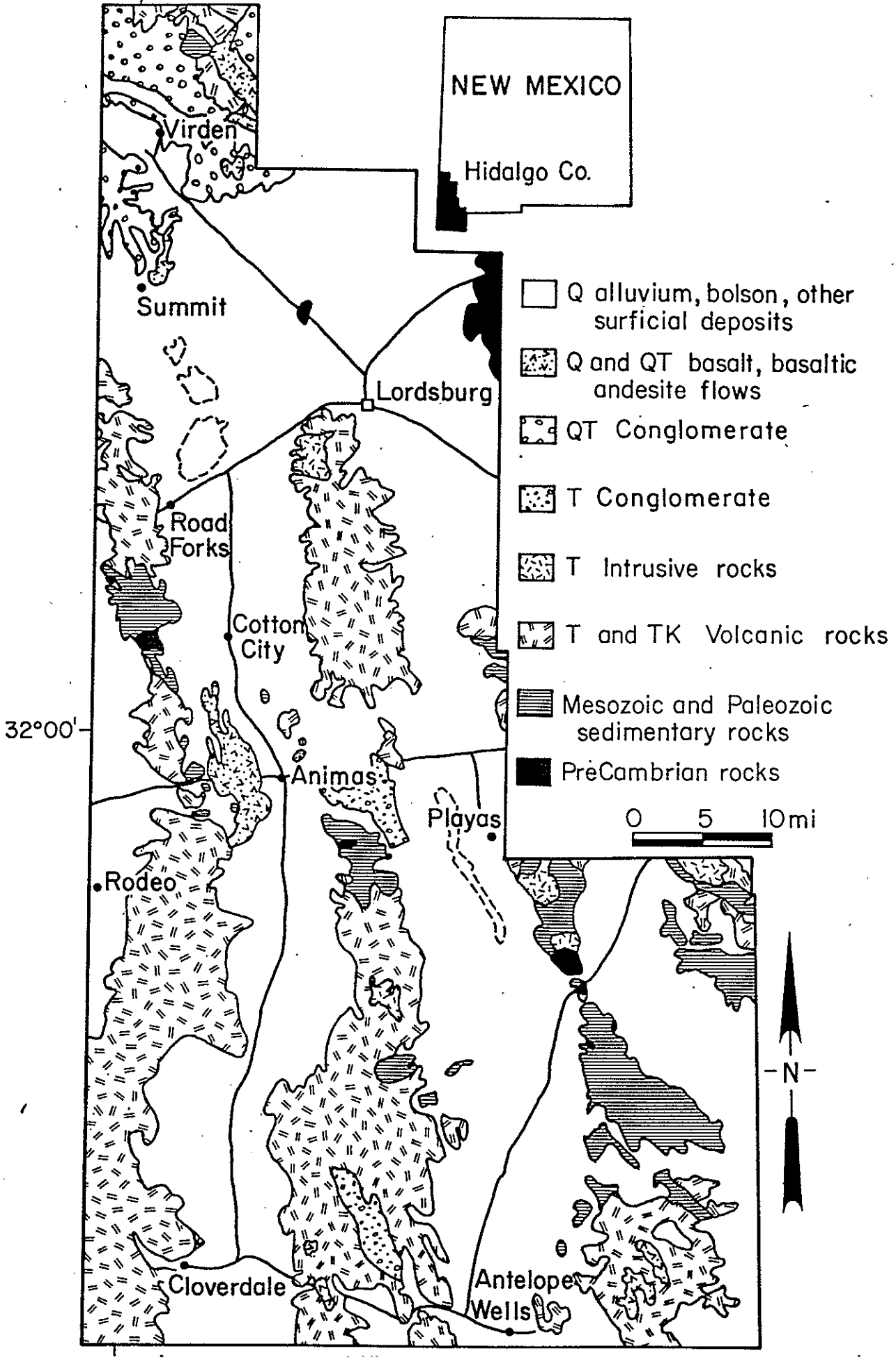

Figure 2 Geologic map compiled from Dane and Bachman (1965), Clemons (1983), Drewes and Thorman (1980, 1980a), and Drewes (1982).

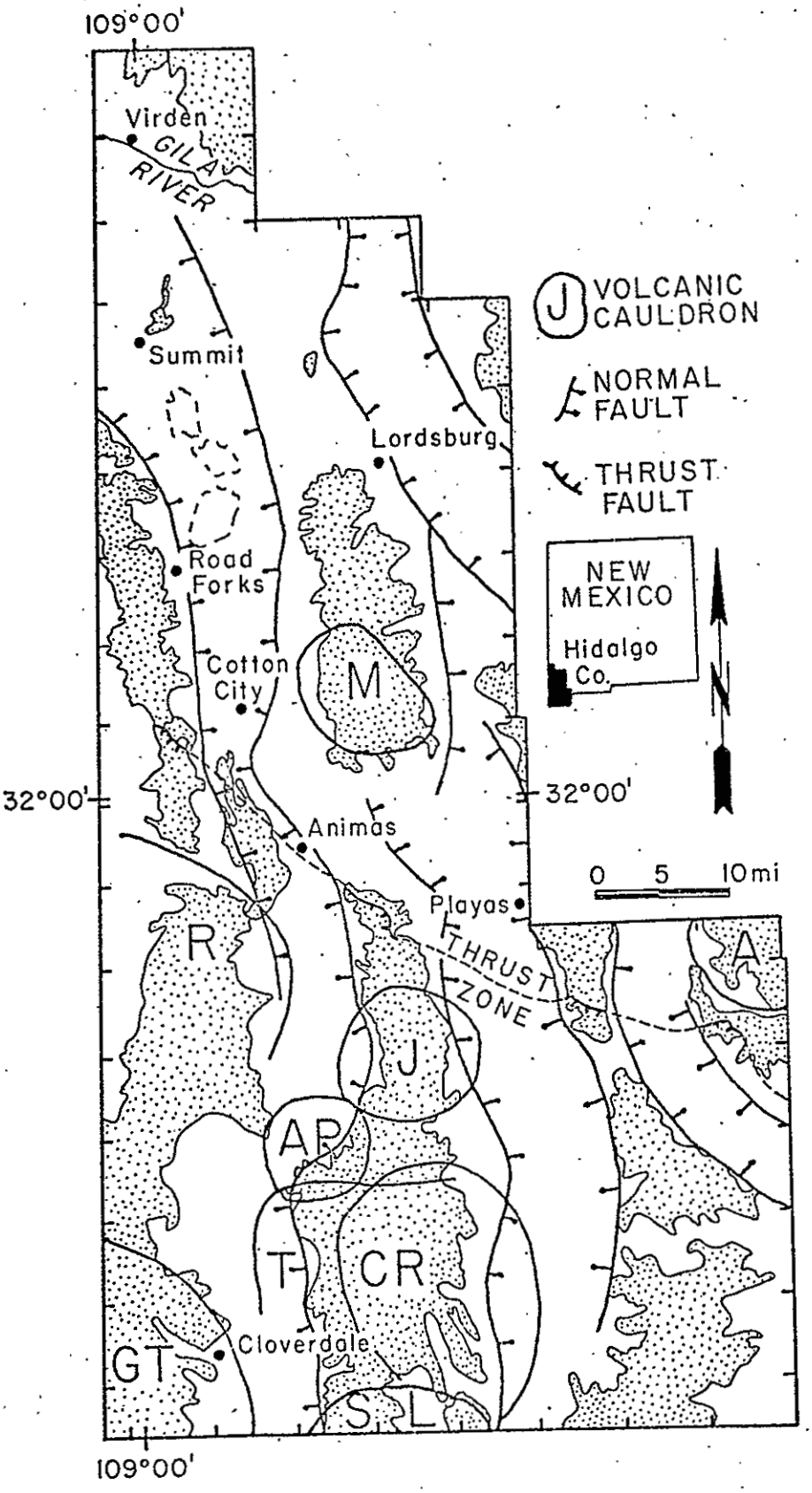

Figure 3 Tectonic and volcanic features compiled from Elston et al. (1979), Thompson (1981), and Lohse (1981).

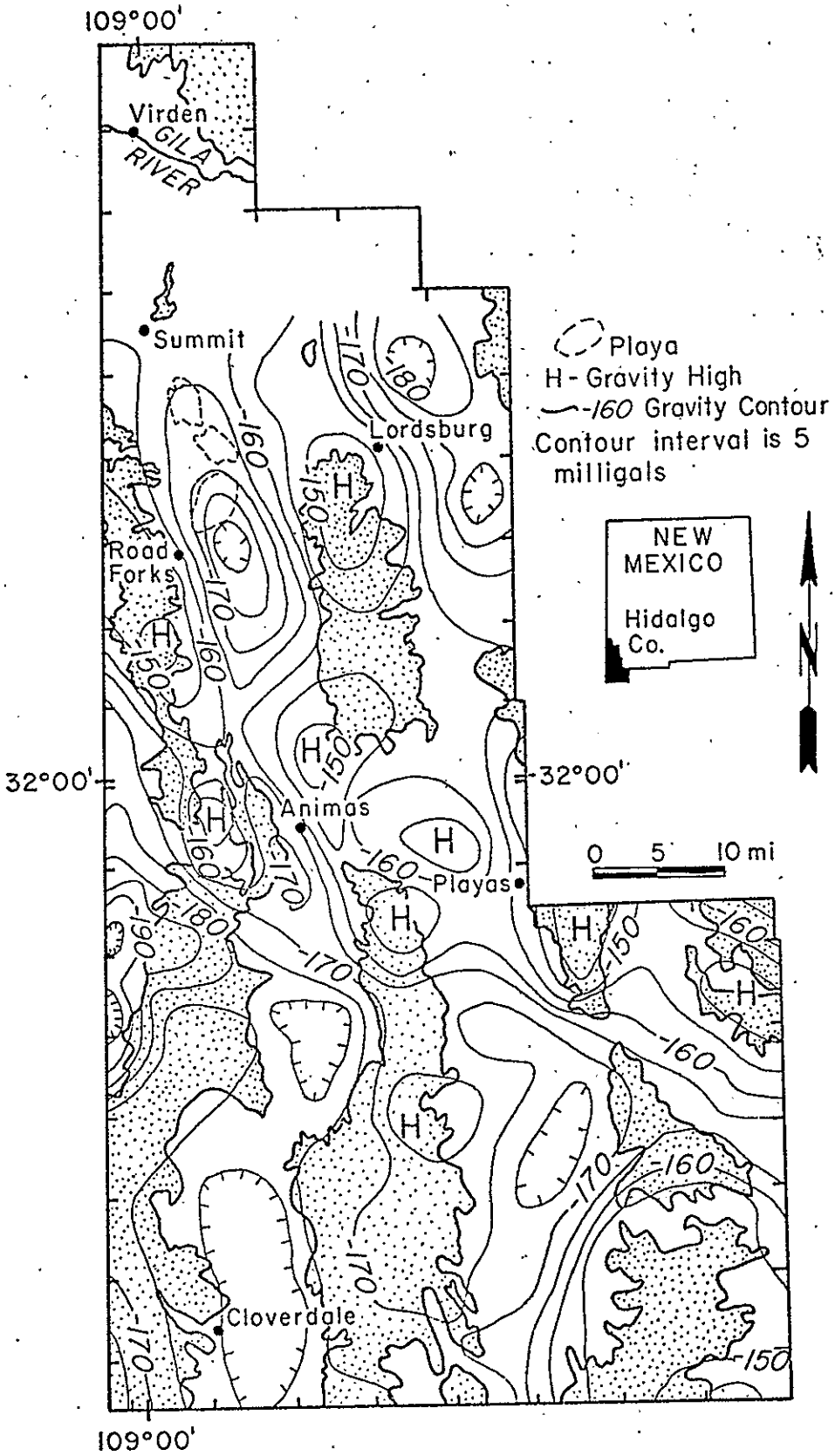

Figure 4 Complete Bouguer gravity anomaly map (5 milligal contour interval) from Lance et al. (1982)

mi (13 km) wide, 50 ft (15 m) deep, and covered an area 150 sq mi (390 sq km).

Geophysics

Numerous geophysical data help define the tectonic and volcanic features in the Animas Valley. These include a 5-milligal (mgal) complete Bouguer gravity anomaly map (Lance, et al., 1982), a 2.5 mgal complete Bouguer gravity anomaly map (Wynn, 1981), and three seismic-refraction profiles (Hans Ackermann, written communication, 1982).

The 5 mgal complete Bouguer gravity anomaly map shows the valley to consist of a series of elongate gravity lows (fig. 4). These lows are interpreted as a series of linked structural depressions similar to those characterizing the Rio Grande rift in the vicinity of Socorro as described by Sanford (1968).

The major gravity low is that situated between Road Forks and Lordsburg (fig. 5). The 2.5 mgal complete Bouguer gravity anomaly map shows that the central portion of this feature is symmetrical in cross section, whereas the northern and southern portions are asymmetrical. The symmetry of the depression signifies the nature of faults along the border of the basin. A gravity low that shows a steep dip from the mountains to the valleys indicates a narrow fault zone with large displacement (distinct density contrast), whereas, a gradual dip indicates step faulting (gradual density contrast) with or without some tilting.

Two series of gravity highs define northwest-southeast and north-south trends of high-density material. The northwest-

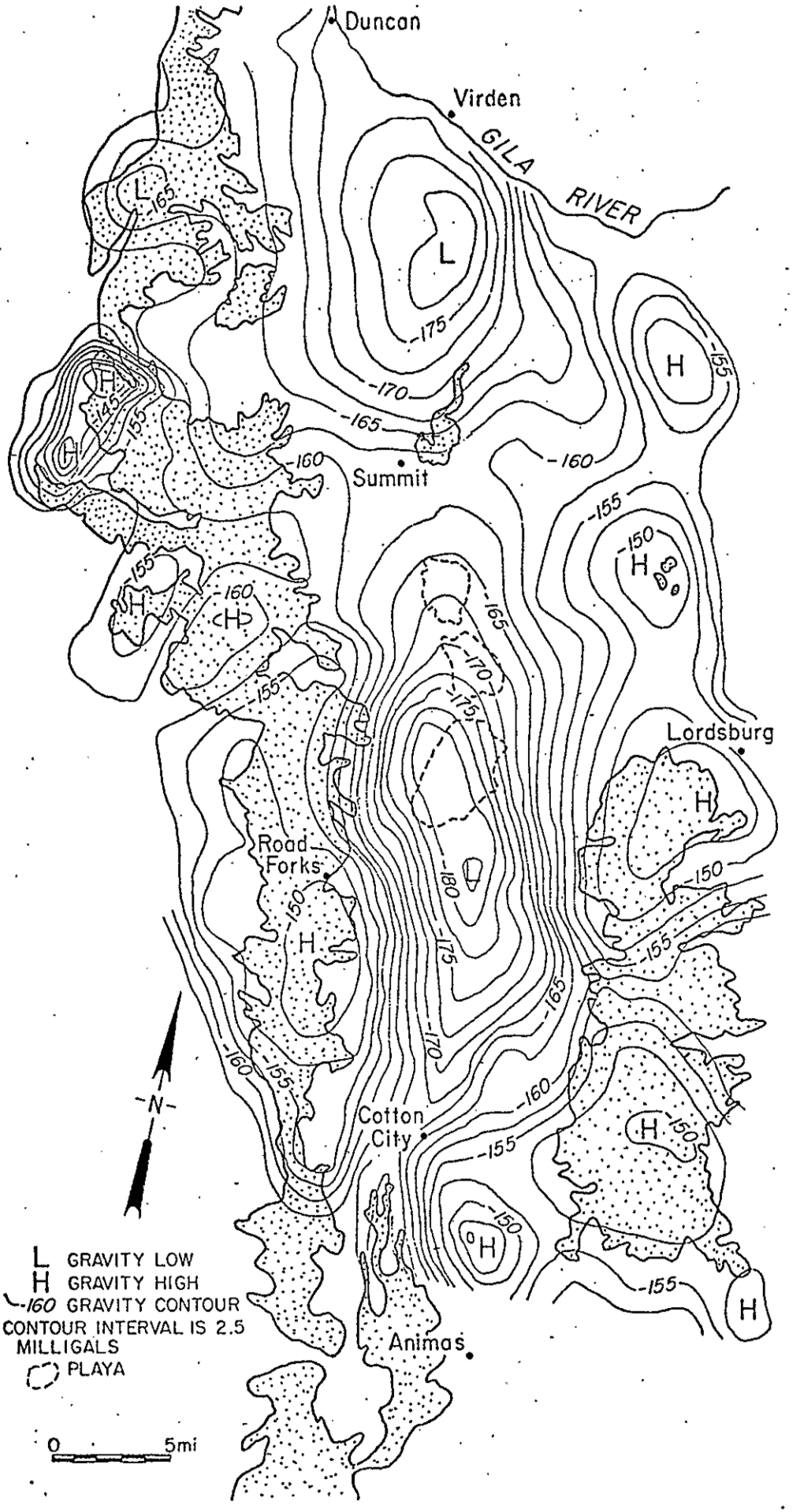

Figure 5. Complete Bouguer anomaly gravity map (2.5 milligal contour interval) from Wynn (1981)

southeast trend of gravity highs is interrupted by a gravity low as the trend crosses the Animas Valley (fig. 4). The superposition of the gravity low on the trend of gravity highs suggests that the northwest-southeast trend of gravity highs is older than the north-south trend of gravity highs.

Seismic-refraction data were purchased and interpreted by the U.S. Geological Survey for the Southwest Alluvial Basins Project (Hans Ackermann, written communication, 1982). As shown herein, seismic refraction profiles (figs. 7, 8 and 9) reflect reinterpretations by the authors. Generally, seismic velocities greater than 10,000 to 11,000 ft/s indicate a dense, low-porosity geologic unit that would not yield significant quantities of water to wells.

Location of seismic-refraction profiles is shown in figure 6. Profile number 4 is oriented east-west and indicates the nature of the bordering faults in the vicinity of the town of Animas (fig. 7). At this point in the basin, the border faults are high-angle normal faults with an indeterminate amount of throw. Profile number 5 is also oriented east-west and shows the bordering faults in the vicinity of Cotton City to consist of a series of step-faults (fig. 8). The nature of the bordering faults as defined by seismic- refraction profile numbers 4 and 5 and by cross-sections constructed across complete Bouguer gravity anomaly maps (figs. 4 and 5) at the locations of profile numbers 4 and 5 is similar.

Subsurface Geology

The geomorphology of Lower Animas Valley provides clues to

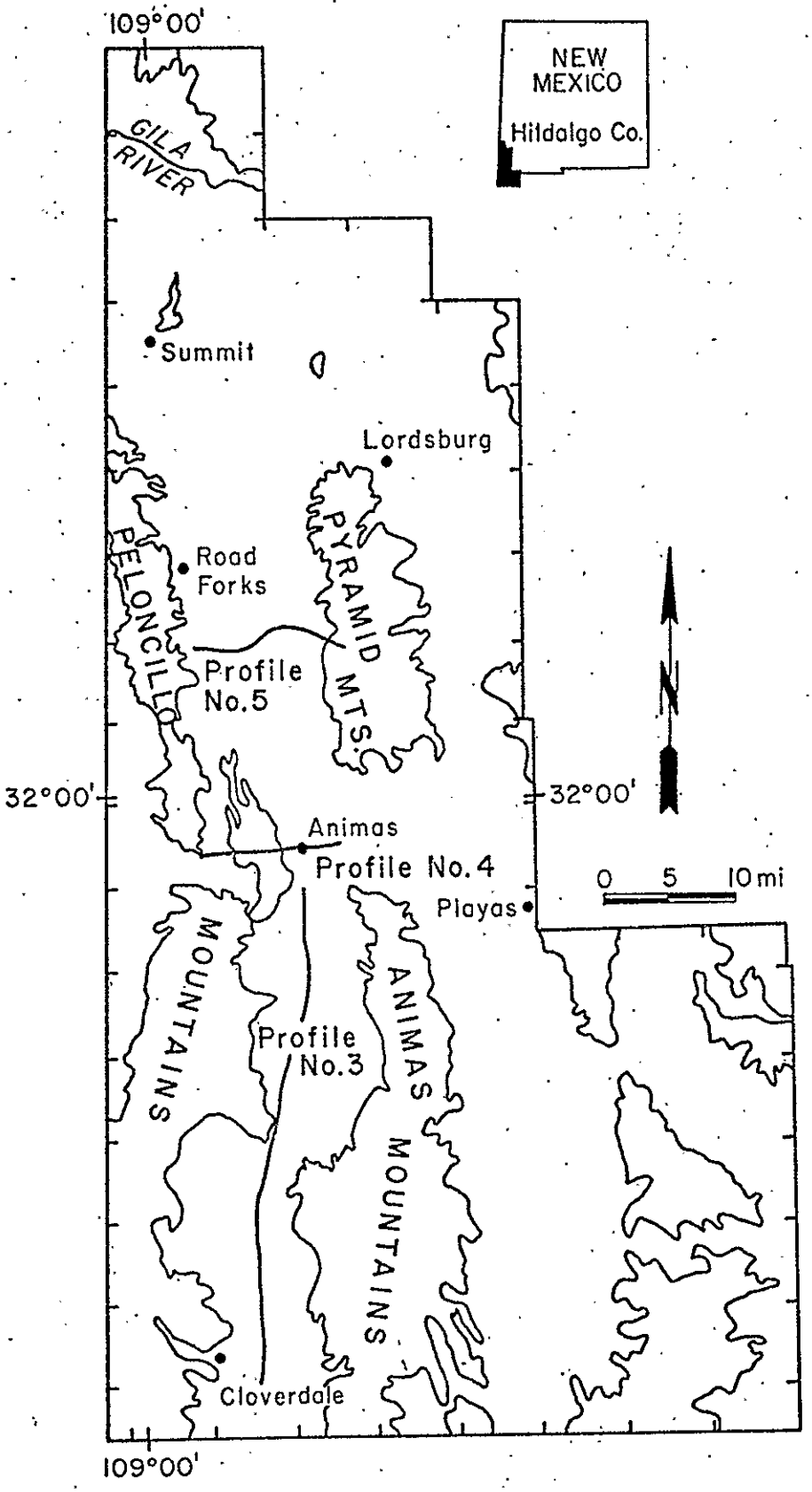

Figure 6. Location of seismic refraction profiles

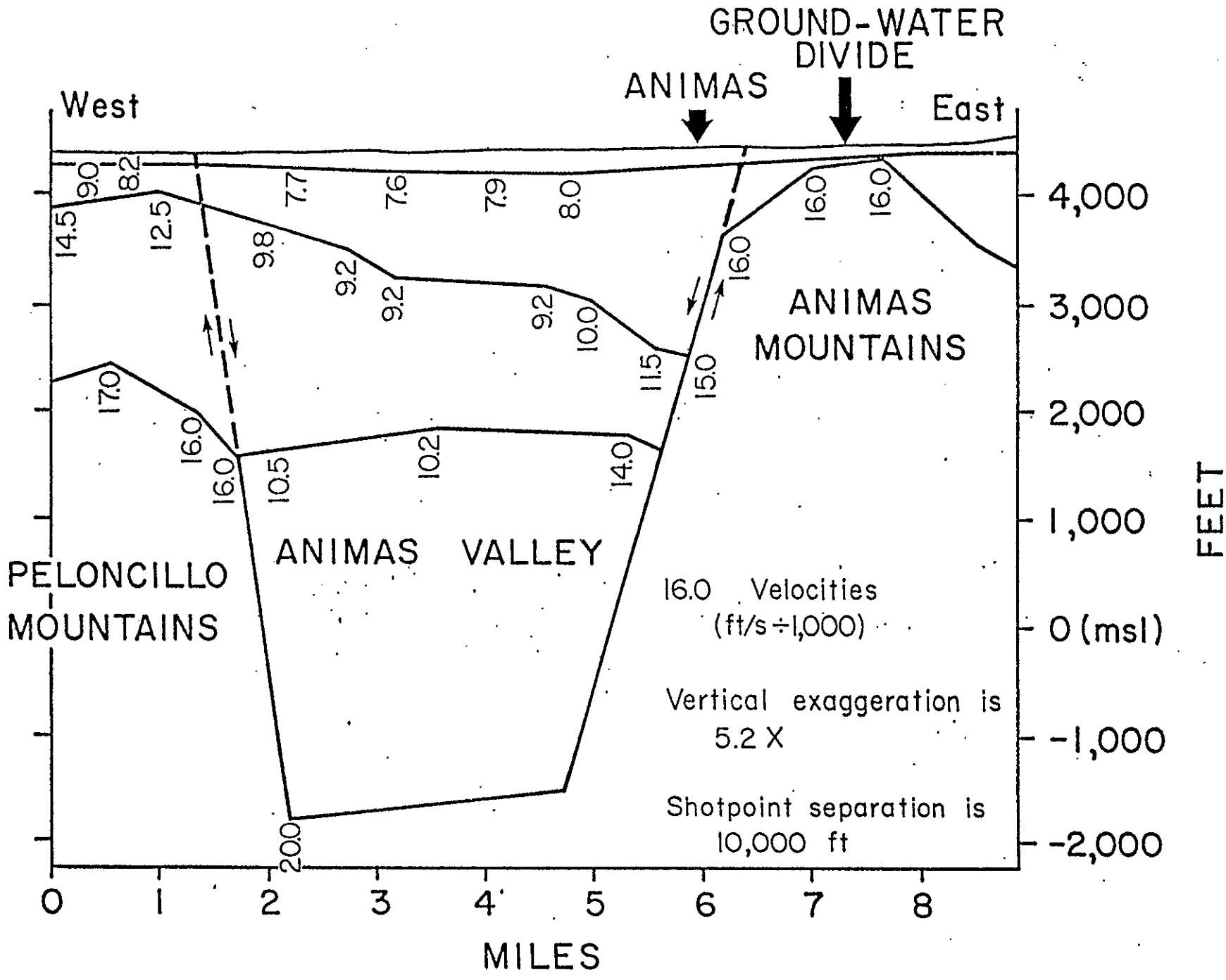

Figure 7. Seismic refraction profile #4.

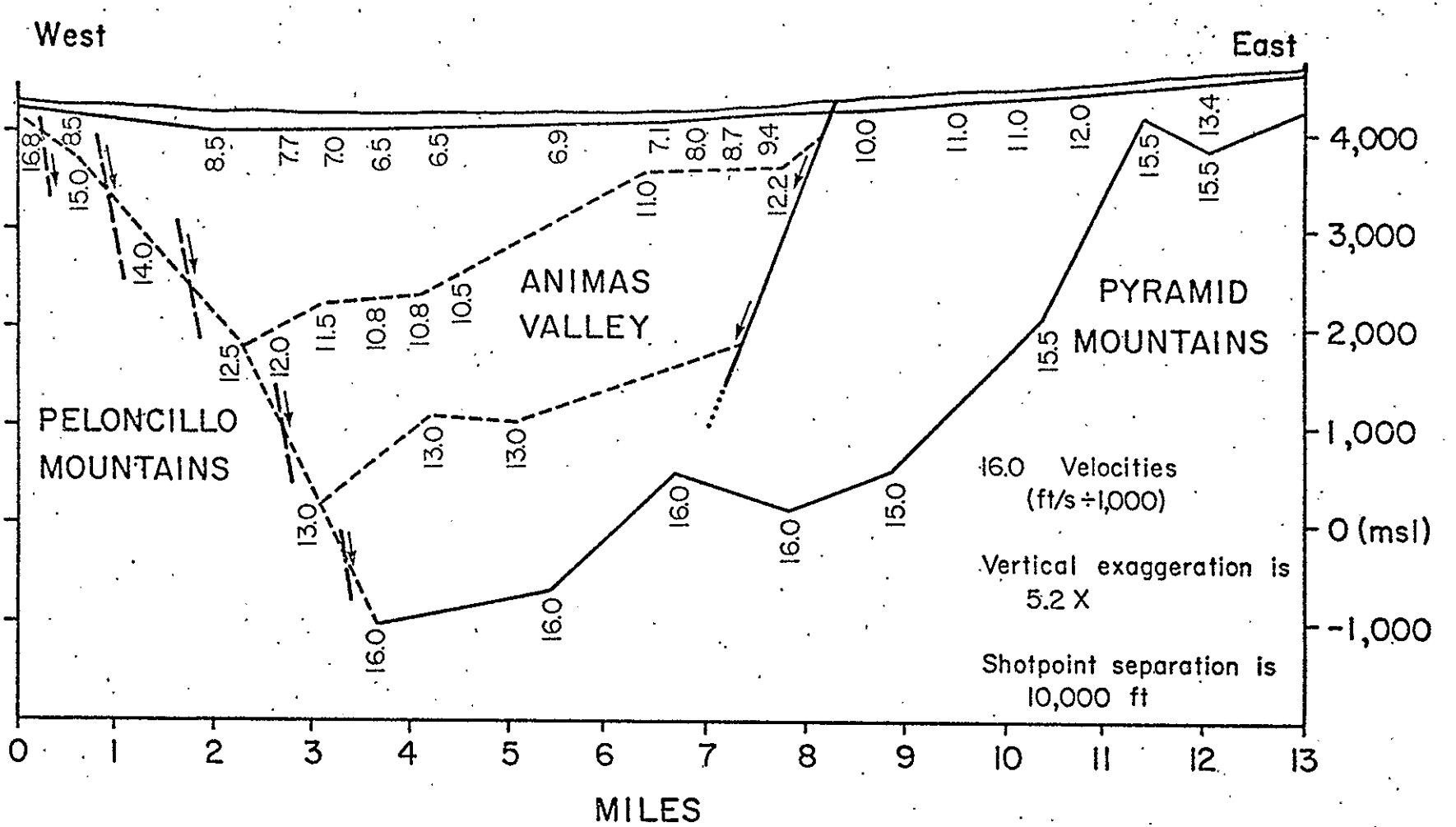

Figure 8. Seismic refraction profile #5

the composition of basin-fill. The compilation of subsurface data reveals in geologic cross-section A-A' a near surface horizon of clay that represents deposition from Lake Animas (O'Brien and Stone, 1982b). Other clay units shown in cross-section A-A' are poorly correlated and probably represent basin-center facies deposition. Basin-fill is composed of a heterogeneous mixture of clay, silt, sand and gravel.

The thickness of basin-fill determinable from geologic, gravity, refraction, and petroleum data is 5,000-6,000 ft (1.5-1.8 km). Of greater importance to the study is the thickness of water-bearing sediments. Refraction profiles 3, 4, and 5 reveal 760 ft (200 m), 2,600 ft (800 m), and 2,000 ft (600 m) of potential water-bearing sediments, respectively. The thickness of potential water-bearing sediments shown on profile 3 (fig. 9) is much less than that shown on profiles 4 and 5 (figs. 7 and 8). Apparently, potential water-bearing sediments in the Upper Animas Valley have been eroded by Animas Creek and redeposited in the Lower Animas Valley. The coarsest sediments transported by Animas Creek would be deposited at the southern (upstream) end of the Lower Animas Valley where there is a decrease in the slope of the land surface (O'Brien and Stone, 1981, Plate 3).

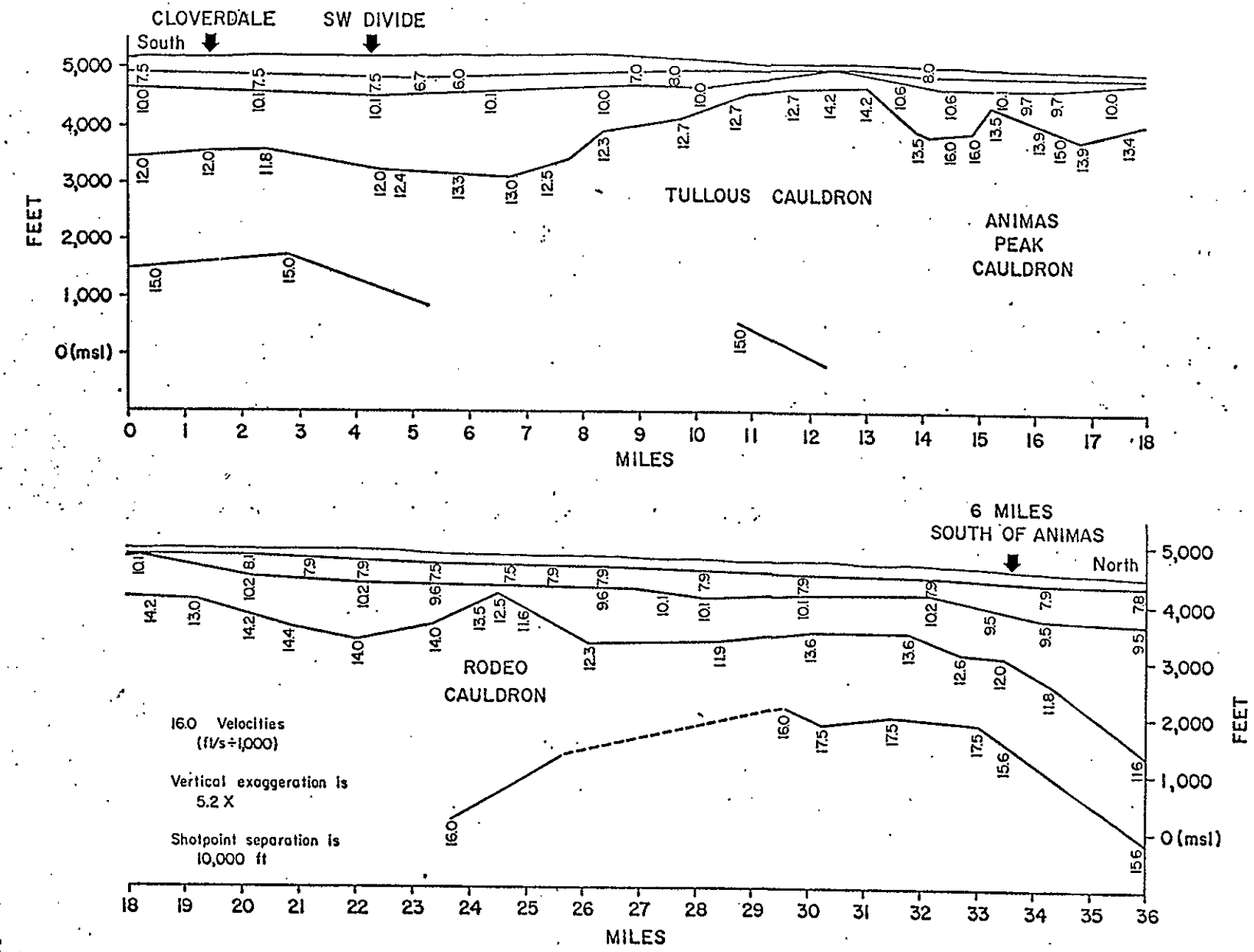

Figure 9. Seismic refraction profile #3.

HYDROLOGIC SETTING

Ground-Water Flow System

Large-scale ground-water withdrawals began during the 1948 irrigation season and disrupted the dynamic equilibrium of the ground-water flow system. Thus, water-level data collected prior to April 1948 were used to define the unconfined hydrologic system at the steady-state condition (O'Brien and Stone, 1981). Steady-state water levels indicate northerly ground-water flow that discharges to the Gila River system (O'Brien and Stone, 1981, Plate 1). A cross section by O'Brien and Stone (1981, Plate 3) shows an abrupt drop in water-level elevation six miles south of Animas. The cause of this sharp decline is the existence of a perched water zone in the Upper Animas Valley. The main zone of saturation that exists in the Lower Animas Valley has not been located in the Upper Animas Valley. Ground-water development in the Upper Animas Valley is confined to the shallow perched ground-water system existing along Animas Creek (O'Brien and Stone, 1981).

Aquifer Extent

Seismic-refraction profile number 3 indicates an abrupt thickening of unconsolidated sediments six miles south of Animas (fig. 9). Figure 4 shows a gravity low indicating a structural depression in this region. Geologic history suggests that since the main phase of the Laramide orogeny the Upper Animas Valley has been topographically higher than the Lower Animas Valley. This topographic effect causes erosion and transport of sediments from the Upper Animas Valley and subsequent deposition in the

Lower Animas Valley. Consequently, the predominance of coarse-grained sediments and greater thickness of unconsolidated material at the break in slope between the Upper and Lower Animas Valley (fig. 9) creates a distinct difference in the hydrologic character of the aquifer in the two areas (especially transmissivity values). Indirect confirmation of this conclusion is provided by the fact that there are no wells currently penetrating a large saturated thickness of basin fill in the Upper Animas Valley. We concluded on the basis of seismic-refraction profiles, gravity data, geologic history, and well logs that the main zone of saturation in the Animas Valley from which large ground-water supplies could be developed has a southern boundary located approximately six miles south of the town of Animas.

The remaining boundaries of the main zone of saturation in the Lower Animas Valley were defined primarily by means of a 2.5 mgal complete Bouguer gravity anomaly map (fig. 5) and a tectonic features map (fig. 3). The east and west boundaries of the unconfined hydrologic system coincide with the basin margin faults as shown in figure 3. The northern extent of the unconfined system corresponds to the northern extent of the gravity low in the Lower Animas Valley (near Summit) (fig. 5).

The southeastern hydrologic boundary is associated with a low alluvial divide between the Animas and Playas Valleys. Precise location of this boundary is difficult because reported water-level data prior to 1981 in this area are scarce. Ground-water flow directions could not be discerned from the existing

data. Recent development of ground water in this area has provided additional data on the ground-water flow system. Analysis of these additional water-level data indicates the existence of a ground-water divide between the Animas and Playas Valleys. The ground-water divide is probably formed by two intersecting cones of depression that have developed by irrigation pumpage in the Animas Valley and by pumpage for smelting purposes in the Playas Valley. The ground-water divide is situated over a subsurface high shown in seismic-refraction profile number 4 (fig. 7). Water-level data are insufficient to delineate the existence of this divide prior to 1981. Thus, the existence of this divide at the steady-state condition is speculative.

The nature of the eastern boundary of the Animas Valley in the vicinity of Lordsburg is also problematical. Figure 1 shows surface-water drainage into the Lower Animas Valley. Figure 5 indicates that in the subsurface broad intervening areas exist between adjacent gravity highs. These intervening areas of less dense material provide pathways for ground water to move into the Lower Animas Valley from the Lordsburg Valley. Hence, both surface water and ground water from the Lordsburg Valley discharge into the Lower Animas Valley.

Recharge

Recharge in the Animas Valley was assumed to occur solely along mountain fronts. Recharge from irrigation return flow or from precipitation on valley lowlands was assumed to be negligible. Mountain-front recharge values were determined from

the following algorithm derived through regression analysis by Jack Dewey (written communication, 1982):

$$Qa = (Ø.Ø155)\ A^{Ø.8}\ S^{Ø.292}\ P^{1.Ø1}$$

where Qa is mountain-front recharge [ft^3/s],

A is surface-water drainage area [mi^2],

S is slope of principal drainage way [ft/mi], and

P is mean winter precipitation (October 1931 through April 196Ø) [in].

Dewey derived this algorithm from data collected for the Albuquerque-Belen basin. Because evapotranspiration in the Animas Valley is greater than that in the Albuquerque-Belen basin the algorithm was modified. Dividing the calculated mountain-front recharge values by a factor of three gave a reasonable value (Dewey, personal communication, 1982). The results of the recharge calculations, when compared on the basis of percent of mean annual precipitation, are within the range of reported values for similar ground-water basins in the vicinity of the Animas Valley (Table 1).

Hydraulic Properties

Hydraulic parameters describing the nature of the water-bearing, basin-fill material were obtained from previous works. Reeder (1957) reported the results of three aquifer tests. He calculated transmissivity values ranging from 22,ØØØ to 246,ØØØ gpd/ft (2,94Ø to 32,89Ø ft^2/d) and averaging 5Ø,ØØØ gpd/ft (6,685 ft^2/d). Arras (1979) reported the results of one pumping test from which a transmissivity of 26,6ØØ gpd/ft (3,56Ø ft^2/d) was determined. Summers (1967) analyzed water-level changes and

TABLE 1 — Reported Recharge Values for Ground-water Basins Proximal to the Animas Valley

Basin	Drainage Area (mi^2)	Mean Annual Precipitation (in/yr)	Ground-water Recharge (ac-ft/yr)	Percent of Precipitation	Source
	Mountain-Front Recharge Calculations				
San Simon, AZ	309	9	15,000	10	White, Hardt (1965)
Willcox, AZ	550	11	75,000	23	Brown, Schumann (1969)
Cienega, AZ	113	20	6,900	6	Geraghty and Miller (1970)
Cienega, AZ	113	20	4,800	4	Nuzman (1970)
Cienega, AZ	113	20	19,558	16	Kafri, et al. (1976)
Cienega, AZ	113	20	15,700	13	Kafri, et al. (1976)
Animas, NM	112	11	1,180	2	Hawkins (1981)
	Recharge Calculations for Mountain-Front Areas in the Animas Valley				
Peloncillo Mtn	34	9	2,500	16	O'Brien and Stone, this report
Pyramid Mtn	65	11	3,000	8	O'Brien and Stone, this report

pumping rates in the irrigated area of Lower Animas Valley over an 18-year period and determined an average transmissivity of 61,700 gpd/ft (8,250 ft^2/d).

Specific-capacity data compiled by Reeder (1957) can be converted to transmissivity data following a method outlined in Walton (1970). The method utilizes the following equation:

$$Q/s = T/264 \log (Tt/2,693\ r^2S) - 65.5$$

where Q/s is specific capacity [gpm/ft],

Q is discharge [gpm],

s is drawdown [ft],

T is transmissivity [gpd/ft],

S is storage coefficient [dimensionless],

r is nominal radius of well [ft], and

t is time after pumping started [minutes].

Examination of specific-capacity data reveals decreasing values with time (1948-1955). Decreasing values of specific capacity are usually caused by partial penetration, well loss, and presence of hydrogeologic boundaries. Specific-capacity data of the greatest magnitude were chosen from the data to avoid these effects.

Storage-coefficient values were reported by Reeder (1957) and Summers (1967). Reeder (1957) calculated an average storage coefficient by dividing the volume of water pumped over the entire valley by the volume of dewatered sediments for the irrigation years 1948 through 1954. He computed storage coefficients ranging from 0.07 to 0.14 and averaging 0.11. Summers (1967) applied a Theis-type solution analysis to the data from the Lower Animas Valley. Water-level data from 1948 to 1966

for wells located four or more miles from the irrigation pumping center were used in his analysis. He computed values of Ø.Ø6 to Ø.Ø7 for storage coefficient. However, Summers assumed that the border faults have no effect on drawdown. This assumption causes his calculated values to underestimate the actual storage coefficient. Therefore, Reeder's (1957) average value of Ø.11 was taken to be representative of the storage coefficient of the water-bearing material in the Animas Valley.

DESCRIPTION OF MODEL

Computer Code

A FORTRAN IV computer code developed by the U.S. Geological Survey (Trescott et al., 1976) was chosen to simulate in two dimensions ground-water flow in the Animas Valley because vertical ground-water flow was assumed to be insignificant. The code offers a numerical approximation to the ground-water flow equation by means of the finite-difference technique. Three solution algorithms are available for solving the simultaneous equations generated by the finite-difference approximation. The solution algorithms include the strongly implicit procedure, the iterative alternating direction implicit procedure, and the line successive overrelaxation method. The strongly implicit procedure was chosen because it generally requires less computer time and has fewer numerical difficulties.

Program options allow simulation of the ground-water flow system as a confined, unconfined, or combined (confined and unconfined) system. Although the ground-water flow system in the Lower Animas Valley is generally an unconfined system, it was simulated as a confined system. Simulation of an unconfined system requires specification of the lower surface of the water-bearing system. Since the lower surface of the basin-fill is poorly known, errors associated with simulation of the system as unconfined were felt to be greater than errors associated with simulation of the system as confined. Jacob (1944) showed that when the saturated thickness of the water-bearing system is much greater than drawdown induced by pumpage, the drawdown in the two

systems will be comparable. In other words, when the percent change in saturated thickness is small, the drawdown in unconfined and confined systems will be comparable. Jacob's equation is:

$$S_a = S_{wt} - \frac{S_{wt}^2}{2m}$$

where Sa is drawdown which would occur in a confined system,

Swt is observed drawdown in unconfined system, and

m is initial saturated thickness of water-bearing system.

Area Modelled and Grid

The ground-water flow system in the Animas Valley was simulated from a point six miles (10 km) south of the town of Animas to a point four miles (6 km) north of Summit. The area in which flow was simulated is bounded on the west by the border fault along the front of the Peloncillo Mountains and on the east by the border fault along the fronts of the Animas and Pyramid Mountains. The simulated area encompassed the main zone of saturation as defined in the hydrologic setting.

A block-centered grid was constructed along the axis of the Lower Animas Valley (fig. 10). The area chosen for simulation was discretized into one-mile-square blocks. The amount of detail in the data did not warrant the use of smaller blocks. The total area covered by the simulation was 457 sq mi.

Model boundaries can be either constant-head or constant-flux. A constant-flux boundary with the flux equal to zero indicates a no-flow boundary. The north, northwest, and northeast boundaries in the modelled area are represented by constant-head nodes (fig. 10). The south, east, and west

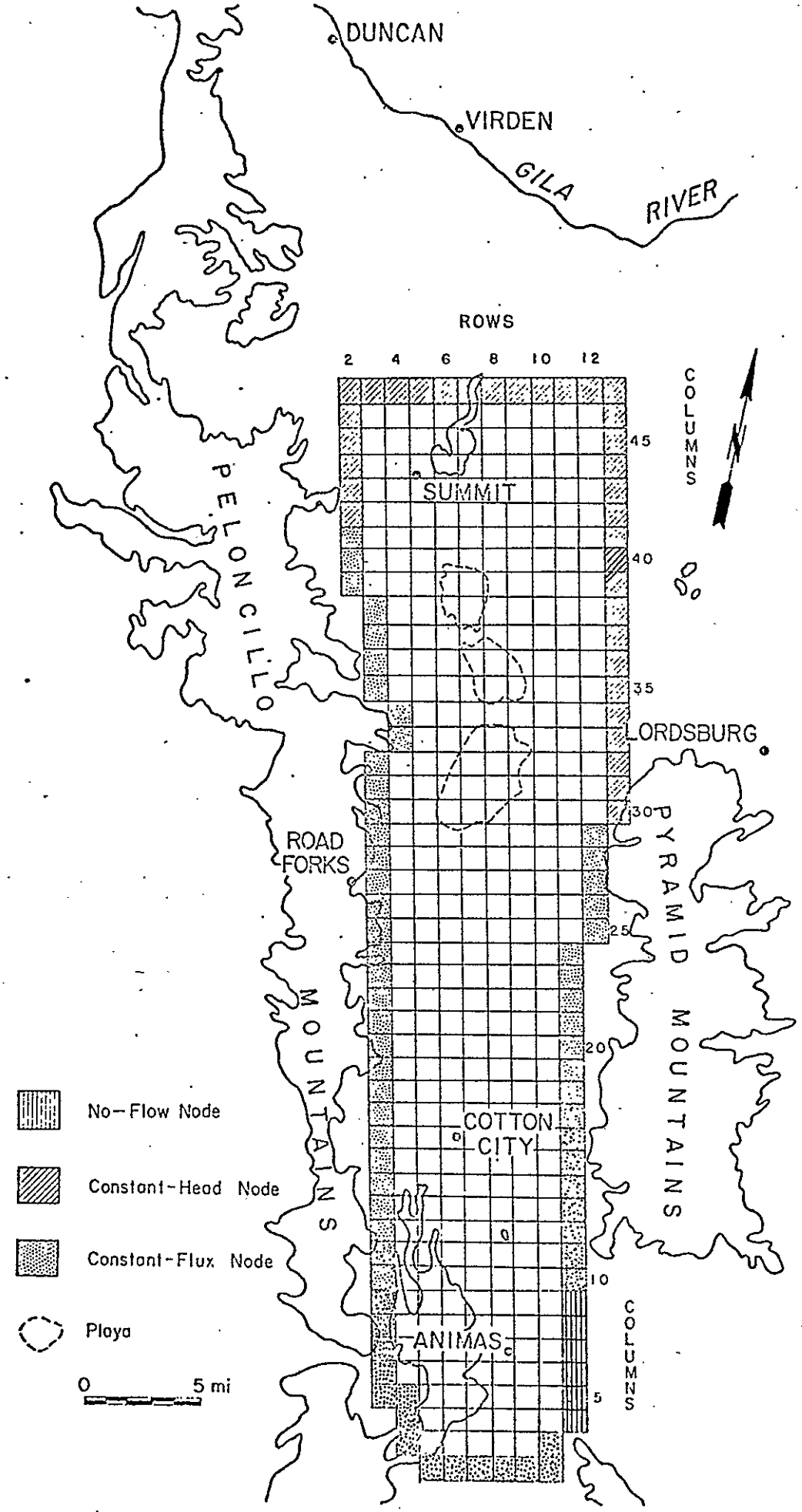

Figure 10. Finite-difference grid and boundary conditions.

boundaries are approximated as constant-flux nodes and the southeast boundary is represented by no-flux nodes (fig. 9). Overall, there are 64 constant-flux, 34 constant-head, and 6 no-flux nodes simulating the boundary conditions of the modelled area.

Constant-head nodes were assigned to nodes distant from the major pumping center and along the northern boundary of the modelled area (fig. 10). The major pumping center is located at Cotton City (fig. 2). In this way, specification of the amount of ground-water flux entering or exiting the system was determined by the computer code. This method of determining flux values was felt to be more accurate than computing constant-flux values because of the existence of water-level data at boundaries of the simulated area.

Mountain-front recharge values were determined from the algorithm of Dewey (personal communication, 1982) as described above. Constant-flux values were assigned to nodes bordering mountain fronts in the vicinity of the pumping center in amounts proportional to the calculated mountain-front recharge occurring adjacent to boundary grid blocks (fig. 10). Constant-flux values assigned to nodes along the southern boundary were determined by initially considering the nodes to be constant-head nodes. Constant-head values were selected from water-level data prior to the 1948 agricultural season. A steady-state simulation was executed and the ground-water flux from the modelled area was recorded. Each node along the southern boundary was changed from a constant-head to a no-flux node, whereupon, a steady-state simulation was executed. The difference in the ground-water flux

from the modelled area after a single node was changed to a no-flux node while keeping the remaining southern boundary nodes as constant-head nodes and the flux when all southern boundary nodes were specified as constant-head nodes was assigned to that no-flux node. The magnitude of the ground-water flux across the southern modelled boundary by this method totalled 4,607 ac-ft/yr. Reeder (1957) computed a value of 2,700 ac-ft/yr as the total flux across the 4,150 water-level contour line (fig. 11). Hawkins (1981) determined the total flow into the Lower Animas Valley from the Upper Animas Valley to be approximately 3,170 ac-ft/yr. The southern boundary flux calculated in this study is 1.7 times Reeder's value and 1.45 times Hawkins' value.

No-flux nodes were assigned to the boundary grid blocks representing the area between the Animas and Pyramid Mountains. No-flux nodes were chosen to approximate the ground-water divide in this area formed by two intersecting cones of depression (fig. 10).

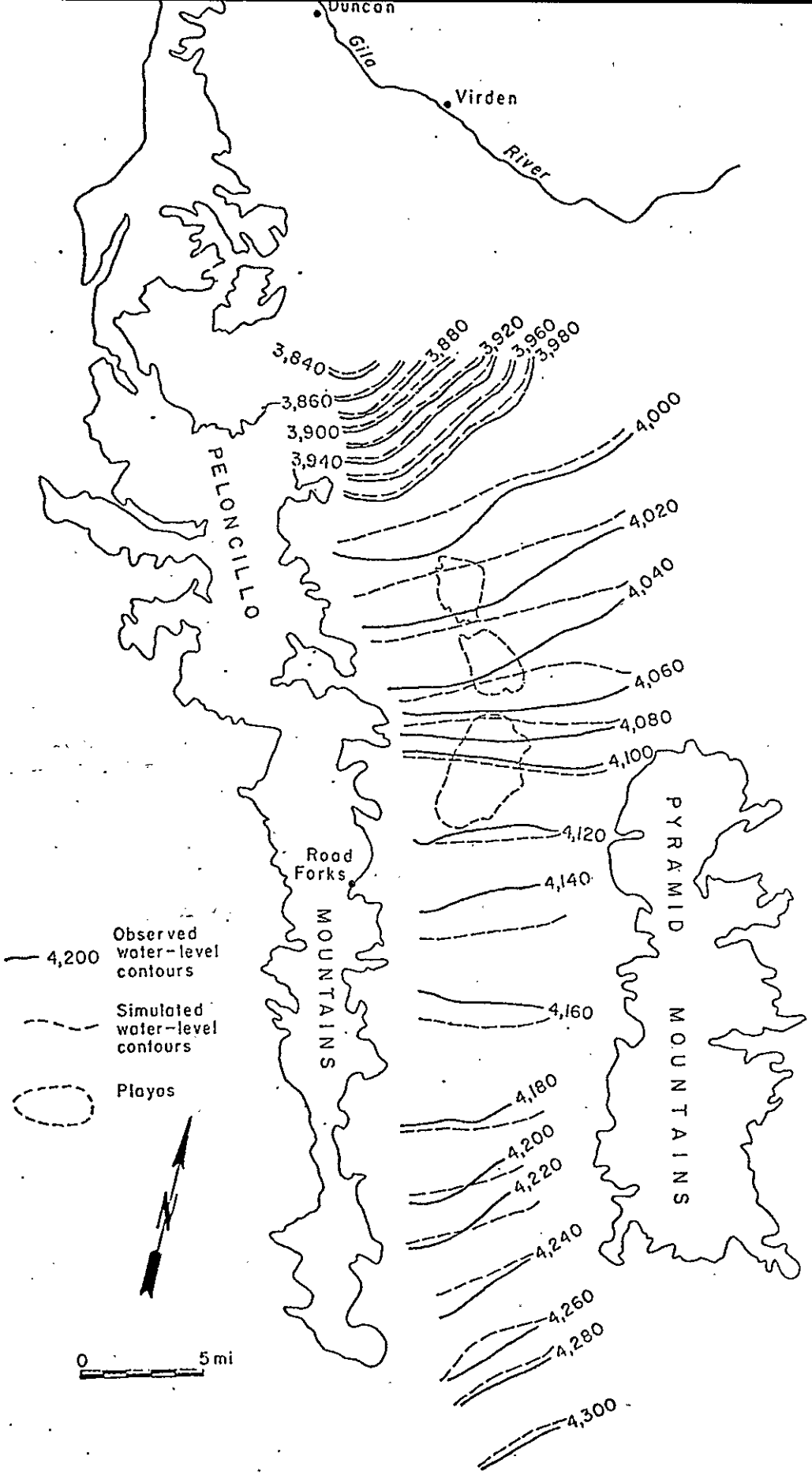

Figure 11. Steady-state water levels (ft) and calibration result (ft). Observed water levels are from Reeder (1957).

STEADY-STATE SIMULATION

Flow Equation

The first step in the modelling procedure was to simulate the steady-state condition of the ground-water flow system. Steady state was defined by water-level data collected prior to large-scale ground-water development for irrigation. Ground-water pumpage for irrigation purposes began during the 1948 agricultural season. This artificial discharge of ground-water terminated the steady-state condition of the flow system.

The two-dimensional, steady-state, ground-water flow equation is:

$$\frac{\partial}{\partial x}\left(T\,\frac{\partial h}{\partial x}\right) + \frac{\partial}{\partial y}\left(T\,\frac{\partial h}{\partial y}\right) = W(x,y,t)$$

where x and y are the Cartesian coordinate axes in the horizontal plane

h is hydraulic head [L],

T is transmissivity [L^2/t], and

W(x,y,t) is the volumetric flux of recharge per unit surface area [L/t].

Data

Necessary data for the steady-state simulation include boundary conditions, a transmissivity matrix, and a starting head matrix. The boundary conditions were chosen as previously described, and the starting head matrix was chosen from existing water-level data (O'Brien and Stone, 1981).

The transmissivity matrix was determined from reported pumping and specific capacity tests, as well as complete Bouguer gravity anomaly maps in combination with well log data. The

spatial distribution of these values was limited primarily to Range 20 west, Townships 25 and 26 south (fig. 1). In order to overcome this data deficiency, the following parameter estimation scheme was developed. Transmissivity values were approximated utilizing aquifer thickness from gravity data and estimated hydraulic conductivity from well-log data. In grid blocks where transmissivity values were available, the relationship between aquifer thickness and hydraulic conductivity was observed. In grid blocks where transmissivity values were not available, the observed relationship between aquifer thickness/hydraulic conductivity and transmissivity was used to estimate transmissivity values.

Calibration

Steady-state calibration was considered to have been achieved when simulated nodal head values were within 25 ft of observed nodal head values. The head matrix computed from the initial execution of the model produced a fairly good match of the observed field values (fig. 11). Transmissivity values were adjusted ±10% until calibration was achieved (fig. 12). Insufficient distribution of observed transmissivity values, uncertainty inherent in published field measurements, and the effects of partially penetrating wells justify adjustment of transmissivity values within a reasonable range. As a check on the resulting transmissivity distribution, the transmissivity matrix was compared to complete Bouguer gravity anomaly maps. The agreement of the transmissivity distribution with the complete Bouguer gravity anomaly maps is quite good (fig. 13).

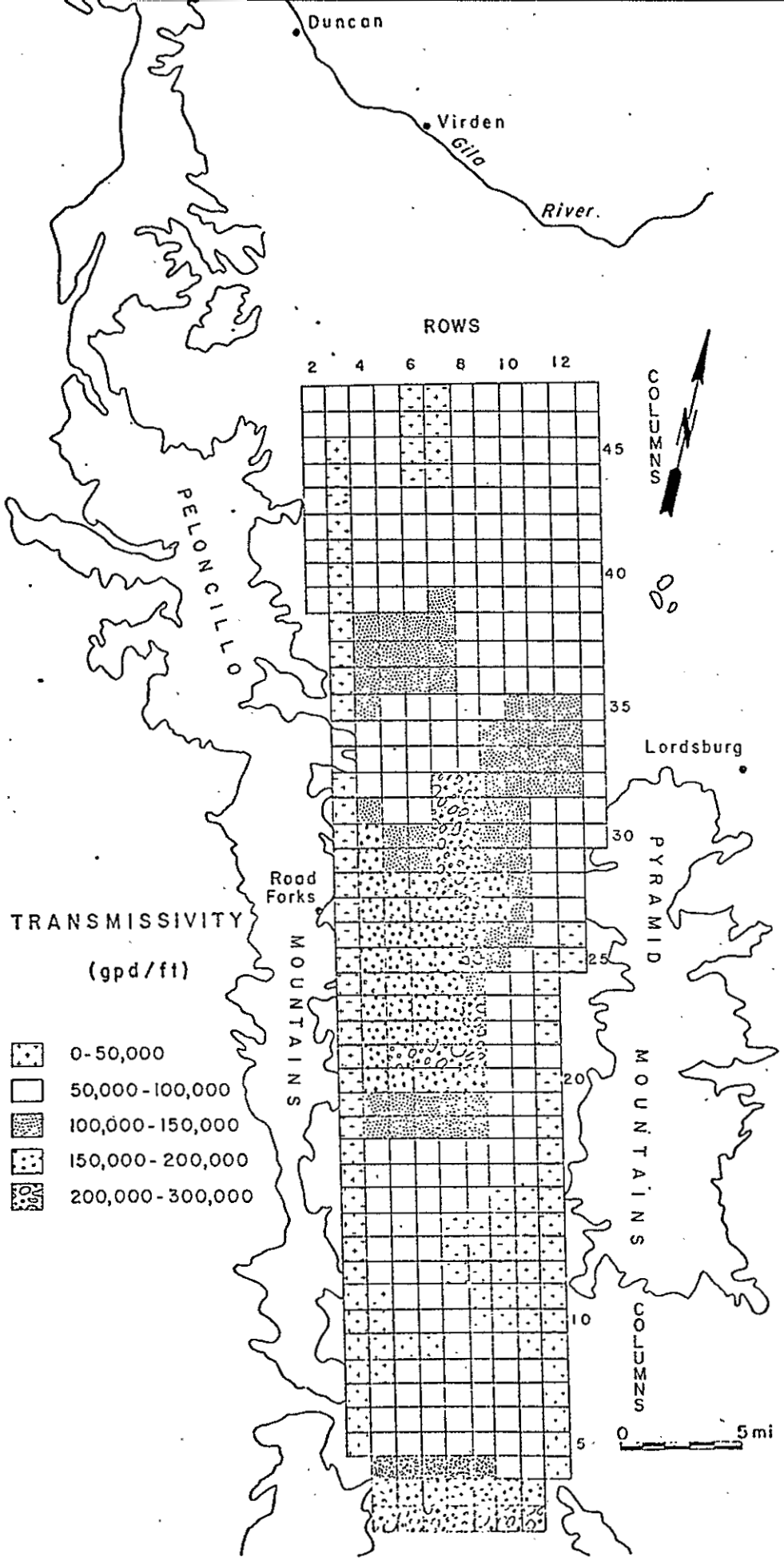

Figure 12. Transmissivity magnitude and distribution.

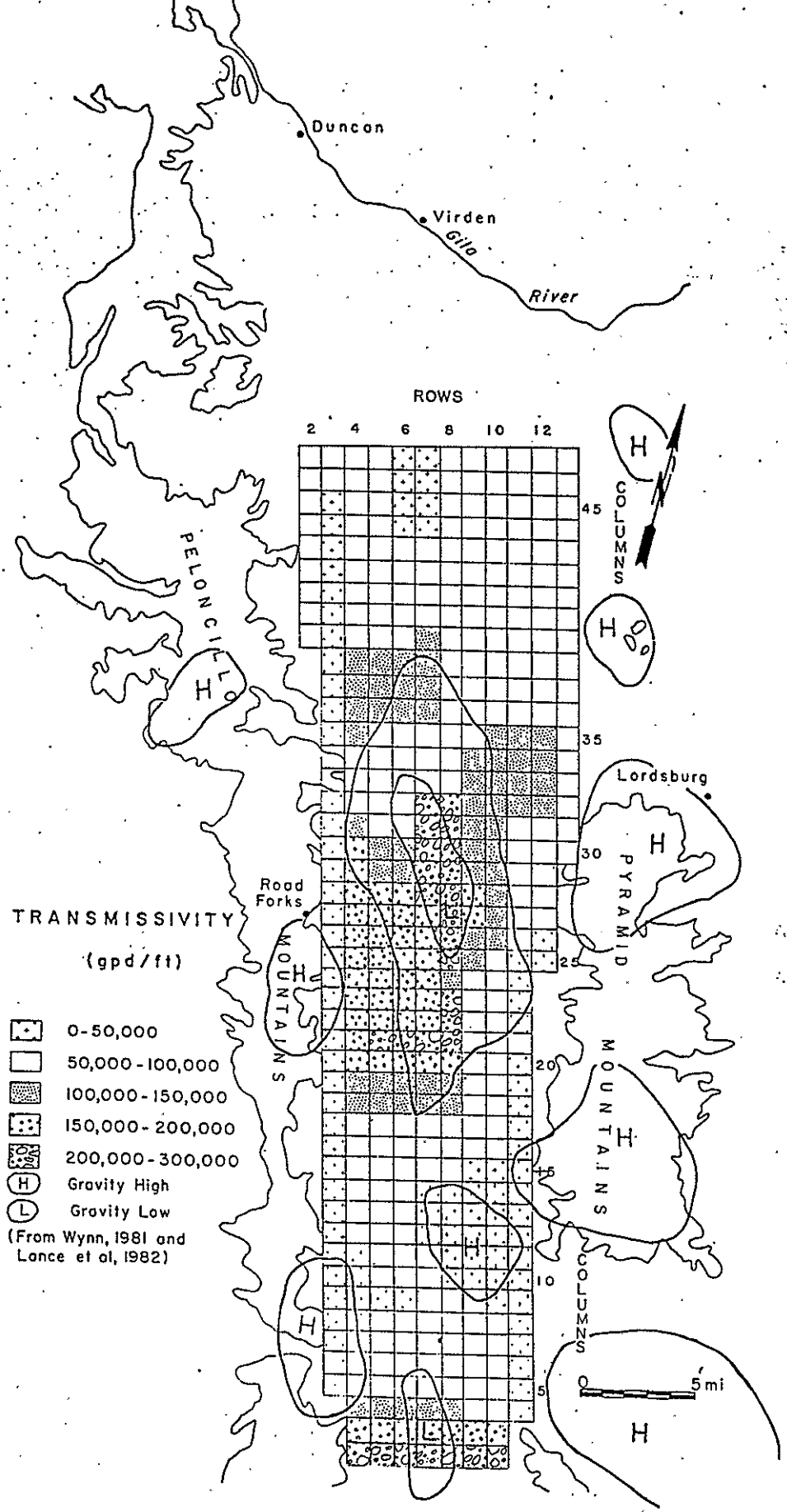

Figure 13. Relationship of gravity data to transmissivity magnitude and distribution.

The total steady-state ground-water flux across the northern boundary of the simulated area was determined by the model to be 12,655 ac-ft/yr. Streamflow gages on the Gila River, roughly bracketing the area to which ground-water from the Animas Valley would discharge, yield streamflow gain values of 21,273, 19,778, and 14,984 ac-ft/yr for the years 1940, 1941, and 1942, respectively. The drainage area contributing to this segment of the Gila River is mostly composed of the Animas Valley. This information provides another indication that the steady-state ground-water flow model of the Animas Valley as conceived is in fair agreement with the observed ground-water flow system.

TRANSIENT SIMULATION

Flow Equation

The steady-state calibration process provided a transmissivity matrix using boundary conditions chosen, and a steady-state head matrix. The two-dimensional, transient, ground-water flow equation is:

$$\frac{\partial}{\partial x}\left(T\,\frac{\partial h}{\partial x}\right) + \frac{\partial}{\partial y}\left(T\,\frac{\partial h}{\partial y}\right) = S\,\frac{\partial h}{\partial t} + W(x,y,t)$$

where x and y are the Cartesian coordinate axes in the horizontal plane,

h is the hydraulic head [L],

T is the transmissivity [L^2/t],

S is storage coefficient [dimensionless],

t is time [t], and

W(x,y,t) is source or sink term [L/t].

Since storage coefficients and ground-water withdrawals are not needed to solve the steady-state case of the ground-water flow equation, a transient simulation was run to calibrate storage coefficients and to verify ground-water withdrawals. Verification of the model was conducted by simulating the ground-water flow system from April 1948 to April 1981.

Data

Additional data for the transient simulation include the storage coefficient matrix and ground-water withdrawals. The average storage coefficient determined by Reeder (1957) was chosen as the storage coefficient value over the entire simulated area. Ground-water withdrawals placed on the steady-state ground-water flow system were compiled from information in the

State Engineers' Office (SEO), Deming. The SEO measured discharge from 27 irrigation wells in September and October, 1948. Farmers reported hours of pump operation to the SEO. Based on discharge rates measured by the SEO and reported duration of pumping, the total volume of ground water pumped during the 1948 irrigation season was estimated. This scheme for determining the magnitude of ground-water withdrawals was utilized for the 1949, 1950, and 1951 irrigation seasons.

In 1951 and 1952, electrically powered motors replaced internal combustion motors on pumps in the Animas Valley. In 1952, the SEO started to estimate total ground-water withdrawals on the basis of electric power records and pump ratings (quantity of water pumped per unit of electric power consumed). This estimation scheme for determining the magnitude of ground-water withdrawals was used for the 1952 through 1959 irrigation seasons.

Ground-water withdrawal data for the Animas Valley were unavailable for the 1960 through 1968 irrigation seasons. In 1969, the SEO renewed their commitment to calculate ground-water withdrawals in the Animas Valley. This effort was limited to the calculation of the magnitude of ground-water withdrawals for individual basins every fifth year. The SEO currently computes ground-water withdrawals primarily on the basis of crop type.

Irrigated acreage for the years 1960 through 1968 is a consistent 12,800 acres (table 2). The reported ground-water pumpage in 1959 and 1969 averages approximately 21,000 ac-ft/yr. Assuming that the relationship between ground-water pumpage and

Table 2 -- Irrigation data for the Lower Animas Valley

Year	Irrigated Acreage	Duration of Season (days)	Ground-water Pumpage (ac-ft)
1947	1,000		1,200
1948	4,000	150	6,400
1949	6,800	180	11,000
1950	7,900	195	15,000
1951	9,000	195	18,000
1952	10,900	195	21,000
1953	11,000	220	24,000
1954	11,400	220	19,500
1955	11,400	195	19,800
1956	12,500	195*	22,700
1957	12,800	195*	19,500
1958	12,800	195*	16,600
1959	12,800	195*	20,900
1960	12,800	195*	21,000*
1961	12,800	195*	21,000*
1962	12,800	195*	21,000*
1963	12,800	195*	21,000*
1964	12,800	195*	21,000*
1965	12,800*	195*	21,000*
1966	12,800*	195*	21,000*
1967	12,800*	195*	21,000*
1968	12,800*	195*	21,000*
1969	11,940	195*	20,180
1970	14,075	195*	21,000*
1971	14,075	195*	21,000*
1972	14,075	195*	21,000*
1973	14,095	195*	15,080*
1974	14,680	195*	15,080*
1975	14,680	195*	15,080
1976	14,680	195*	15,080*
1977	14,680	195*	15,080*
1978	14,680	195*	18,390*
1979	14,215	195*	18,390*
1980	14,210	195*	18,390

* Estimated value

Sources of this information include SEO files, Sorenson (1977), Reeder (1957), Reeder et al. (1959, 1960), and Brian Wilson (personal communication, 1982).

irrigated acreage remained constant during the intervening period, a value of 21,000 ac-ft was selected as the ground-water withdrawal for the 1960 through 1968 irrigation seasons.

Reeder (1957) constructed maps showing the distribution of irrigated acreage in the Animas Valley for the 1950 and 1955 agricultural seasons. In order to assign ground-water withdrawals to nodes, the grid was superimposed on the irrigated acreage maps. The total ground-water withdrawal within a grid block was determined by the percentage of the total irrigated area in that grid block. This percentage of total irrigated area was then multiplied by the corresponding total ground-water withdrawal for that season. The resulting value was the ground-water withdrawal for the grid block during that agricultural season. Since only two irrigated acreage maps were compiled, the distribution of ground-water withdrawal for other agricultural seasons had to be determined from these two existing distribution patterns.

Agricultural seasons with ground-water pumpage less than 18,500 ac-ft/yr were considered similar to the 1950 agricultural season (15,000 ac-ft/yr), whereas, agricultural seasons with ground-water pumpage greater than 18,500 ac-ft/yr were considered similar to the 1955 agricultural season (19,800 ac-ft/yr). The distribution of ground-water withdrawal for an agricultural season followed the distribution pattern determined for either the 1950 or 1955 agricultural season depending on the magnitude of ground-water pumpage. Hence, the 1950 ground-water withdrawal distribution pattern was used for the 1949, 1950, 1951, and 1973 through 1980 agricultural seasons. The 1955 ground-water

withdrawal distribution pattern was used for the 1952 through 1972 agricultural seasons.

Calibration

A transient simulation was executed for the period from April 1948 to January 1955 because fewer assumptions about the data base are necessary during that period. Calibration was considered achieved when simulated drawdown contour lines were within 10 ft of Reeder's (1957) observed drawdown contours (fig. 14). In order to achieve calibration, the nodal distribution of ground-water withdrawal was moved between adjacent nodes in amounts not exceeding ±10%. The inaccuracy in distributing ground-water withdrawals to nodes justifies the adjustment of ground-water withdrawals between adjacent nodes. The storage coefficient matrix was not altered during the transient calibration.

Verification

Model verification was carried out by simulating the drawdown on the ground-water flow system from April 1948 to April 1981. Ground-water withdrawals for the 1955 through 1980 agricultural seasons were added to the transient data base. The transient data base was not changed during the transient verification. The results of the model verification show that the simulated drawdown contour lines are within 18 ft of the observed drawdown contour lines (fig. 15).

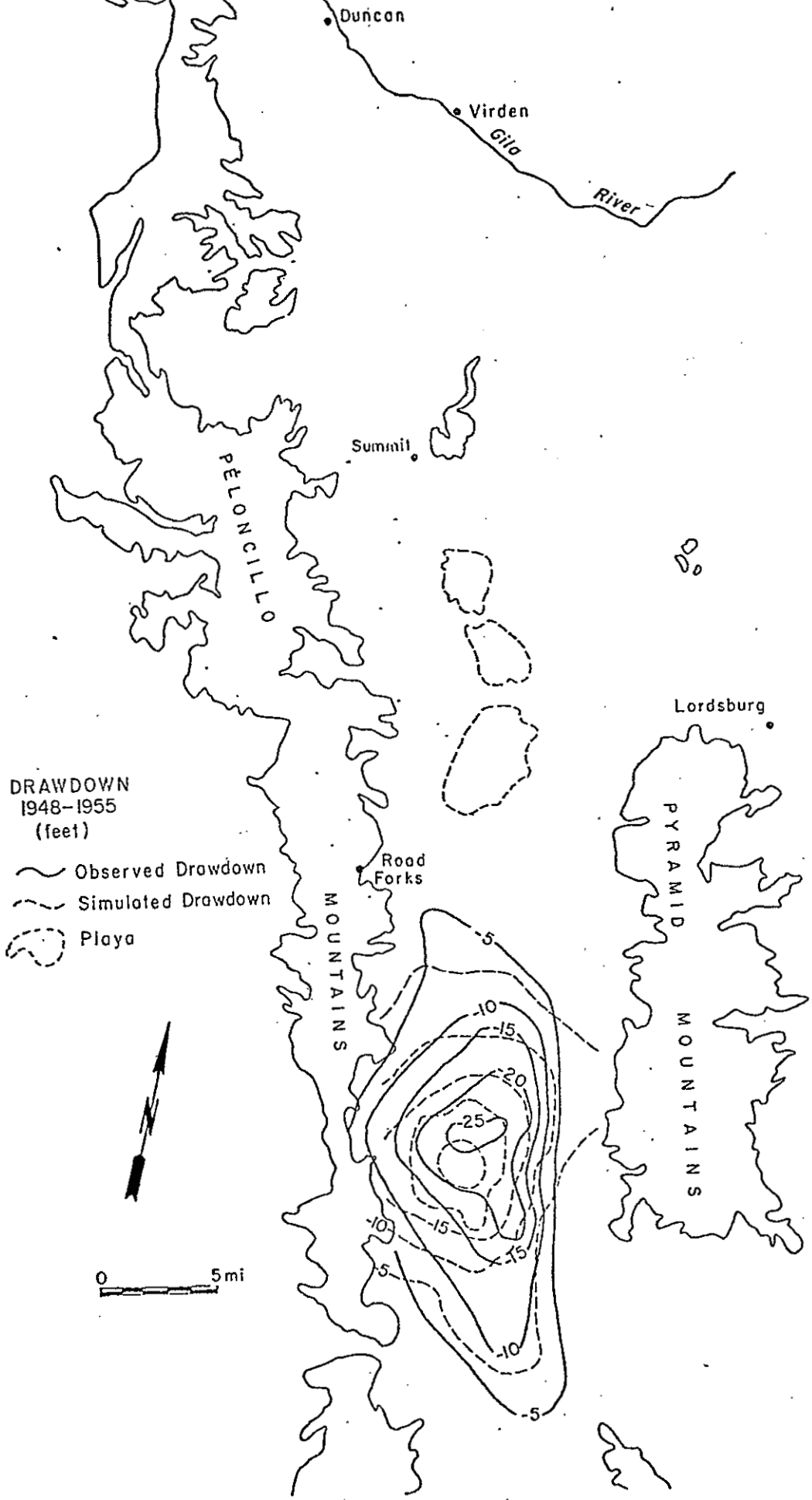

Figure 14. Transient calibration result (April 1948 to January 1955). Observed drawdown from Reeder (1957).

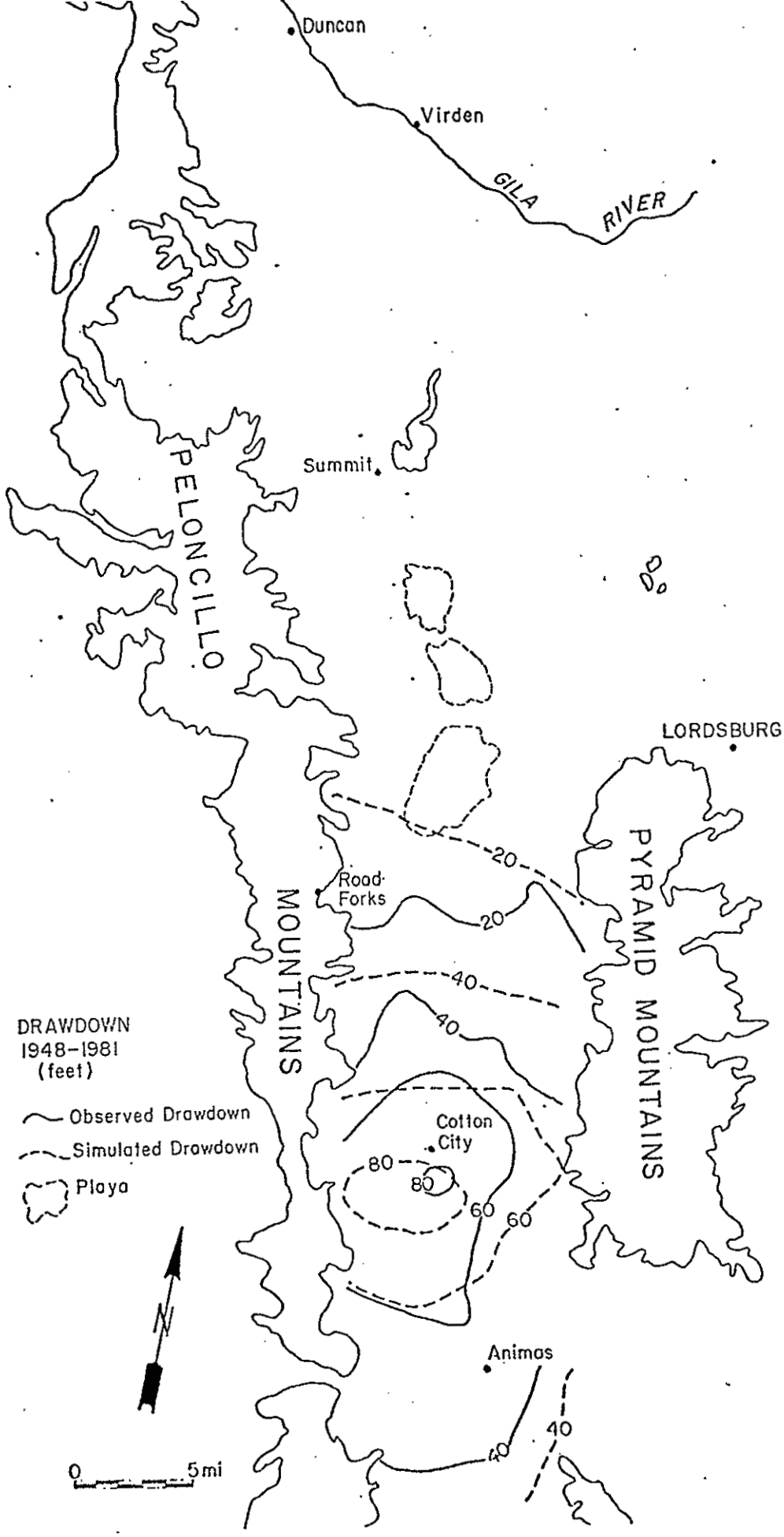

Figure 15. Transient verification result April 1948 to April 1981. Observed drawdown as compiled in this study.

MODEL CONFIDENCE

Sources of Error

The accuracy with which a model simulates historical data provides an indication of the model's ability to project the behavior of a ground-water flow system. Errors in the input parameters, as well as the sensitivity of the model to errors in the input parameters are fundamental factors in model confidence.

The modelling strategy was designed to minimize error in the input parameters. Initially, a steady-state condition was defined. The definition of a steady-state condition permitted inspection and analysis of only two of the four model input parameters necessary for projecting the behavior of the ground-water flow system. The reduction of the number of input parameters reduced the complexity of adjusting four parameters to only two parameters during calibration of the model at steady-state. The result of this strategy was a transmissivity matrix which agreed favorably with the subsurface geology (fig. 13), boundary conditions which, in combination with the transmissivity matrix, produced good agreement with ground-water outflow from the Animas Valley, and a simulated hydraulic head matrix which resembled the observed hydraulic head matrix (fig. 11).

Simulation of the transient ground-water flow system from April 1948 to January 1955 required two additional input parameters. Storage coefficients are poorly known throughout the Animas Valley and an average value determined by Reeder (1957) was used for each node in the modelled area. Ground-water withdrawal records are relatively complete for this period although errors

exist in the total amount and distribution of ground-water withdrawals. The transient simulation from April 1948 to January 1955 involved minor adjustment of the location of ground-water withdrawals. Ground-water withdrawal values were shifted between adjacent nodes in amounts less than or equal to ±10%. The imprecision in assigning both magnitude and location of ground-water withdrawal permits adjustment of these input parameters. Calibration of this transient simulation was considered achieved when simulated drawdown contours were within 10 ft of observed drawdown contours (fig. 14).

Verification of the model involved a transient simulation from April 1948 to April 1981. Input parameters were not adjusted during the verification process. The result of this transient simulation indicates that the model approximates the observed drawdown contours on the ground-water flow system in the Animas Valley to within 18 ft (fig. 15).

The number of unknowns in the simulation of the ground-water flow equation prohibit a unique solution. Hence, more than one combination of input parameters will yield simulated hydraulic head data that suitably match observed hydraulic head data. The model results and model projections could be refined if the following input parameters were better known:

1) Magnitude and distribution of recharge (mountain-front, valley lowland, irrigation return flow, underflow);
2) Magnitude and distribution of transmissivity and storage coefficient;
3) Quantity, duration and areal distribution of ground-water withdrawal;

4) Magnitude and areal distribution of drawdown of the ground-water system.

Sensitivity Analysis

The sensitivity of the model to errors in the input parameters was investigated by perturbing parameters by ±50%. Transmissivity and storage coefficient values were perturbed at all nodes, whereas recharge and ground-water withdrawal values were perturbed only at nodes where these parameters were specified. Each parameter was perturbed by +50% and -50% of its determined value. A computer run, simulating a calendar year, consisted of a 45-day non-pumping period, a 180-day pumping period, and a 140-day non-pumping period. A computer run encompassed 27 time steps and was executed following each parameter perturbation.

The effect on the computed head induced by perturbing a particular parameter was recorded by comparing the computed head values after each parameter perturbation with the computed head values when all parameters were unperturbed. The difference in the computed head values was termed the cumulative error. The cumulative error was defined as the absolute value of the difference in the computed head values summed over all nodes in the modelled area.

Figure 16 illustrates the cumulative error in the computed head values when each parameter was perturbed by ±50% of its determined value. Storage coefficient values perturbed by -50% of their determined values induced the greatest cumulative error. On the other hand, storage coefficient values perturbed by +50%

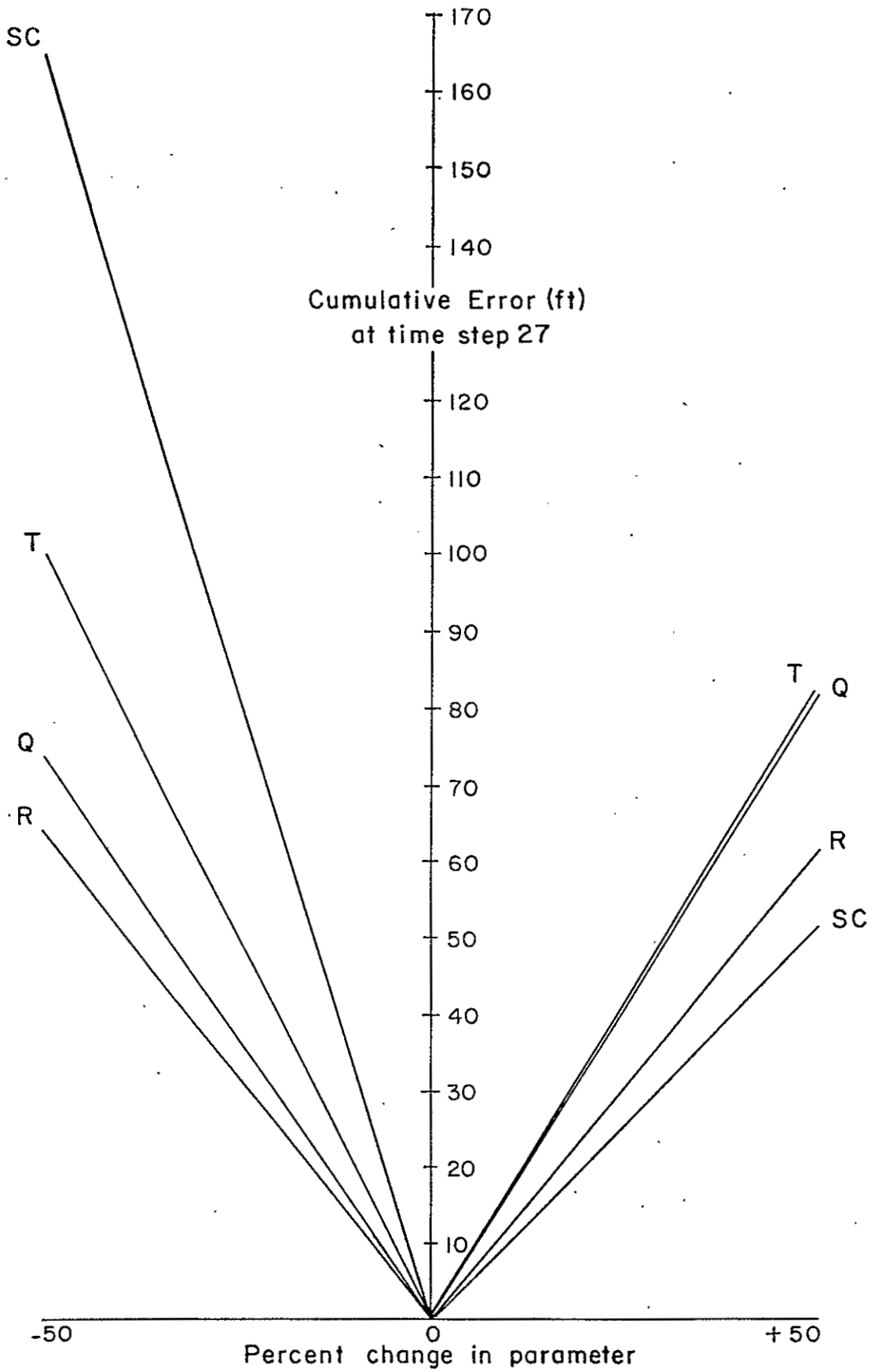

Figure 16. Model sensitivity results for storage coefficient (SC), transmissivity (T), ground-water withdrawal (Q), and mountain-front recharge (R).

induced the least cumulative error. Recharge values perturbed by +50% and -50% induced about the same amount of cumulative error; 61.2 ft and 64.3 ft, respectively. Transmissivity values perturbed by -50% induced 18% more cumulative error in computed head values than transmissivity values perturbed by +50%. Ground-water withdrawal values perturbed by +50% of their determined values induced 10% more cumulative error in computed head values than ground-water withdrawal values perturbed by -50%. Hence, storage coefficient, transmissivity, and recharge values perturbed by -50% of their determined values induced more cumulative error in computed head values than storage coefficient, transmissivity, and recharge values perturbed by +50% of their determined values.

The sensitivity of the model to changes in input parameters was further investigated by perturbing each parameter by -50% and +100% of its determined value. The computed head values after perturbing parameters were graphed versus computed head values when parameters were not perturbed. Cross-sections of head values were constructed along grid columns 11 and 22. Grid columns 11 and 22 have constant-flux nodes at their east and west boundaries (fig. 10). Figure 17 shows the effects of perturbing parameters by -50% and +100% of their determined values. Note that the ratio of the horizontal to vertical scale is 5280 to 2.

Figure 17a illustrates that perturbing transmissivity values causes computed head values to deviate from the determined head values along the east and west boundaries of the cross-section. Computed head values agree with determined head values along the central portion of the cross-section. Figure 17b indicates that

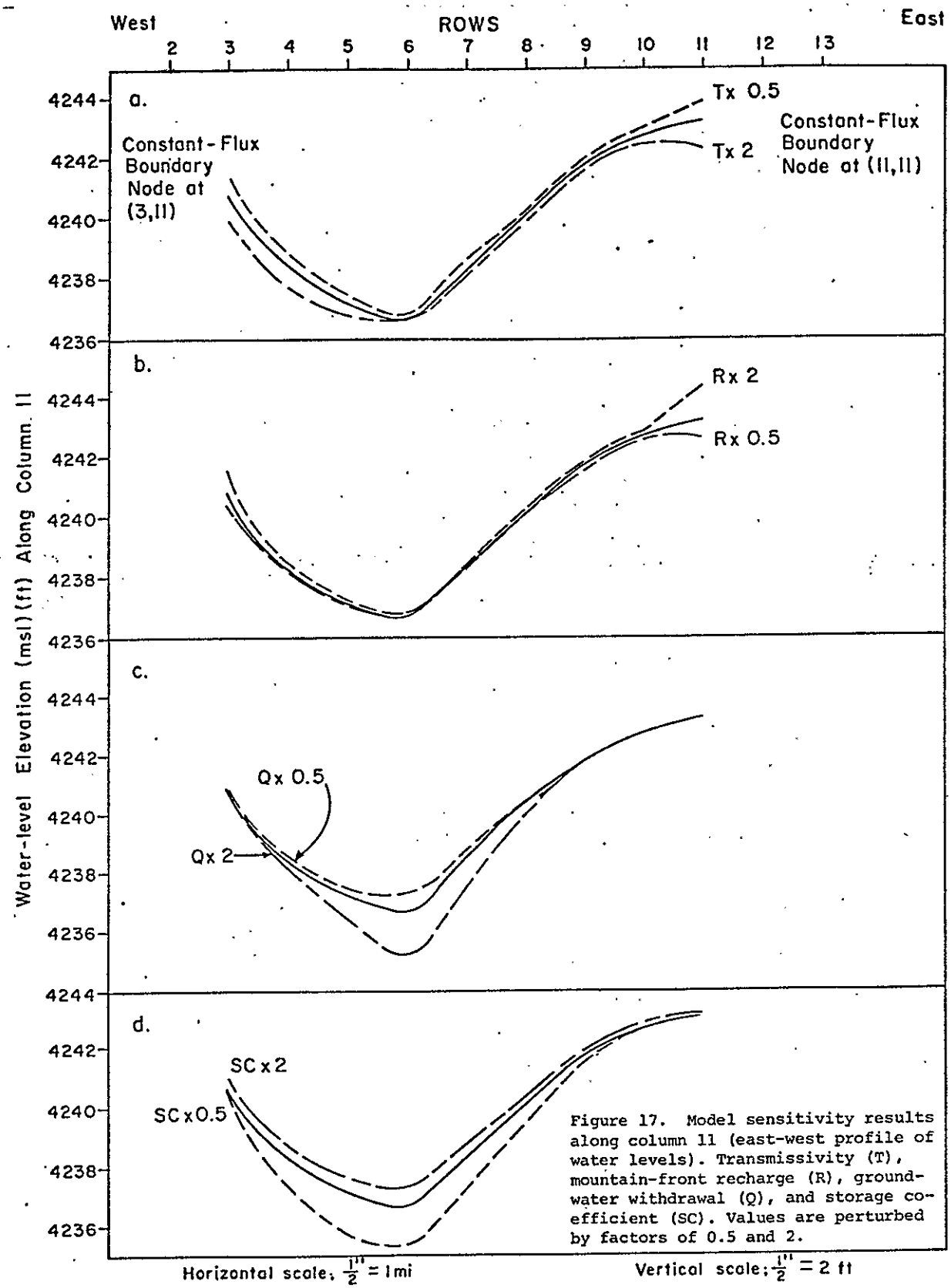

Figure 17. Model sensitivity results along column 11 (east-west profile of water levels). Transmissivity (T), mountain-front recharge (R), groundwater withdrawal (Q), and storage coefficient (SC). Values are perturbed by factors of 0.5 and 2.

perturbed recharge values demonstrate a behavior similar to that of the perturbed transmissivity values. The difference in figures 17a and 17b is that doubling transmissivity values has a similar affect on computed head values as halving recharge values.

Conversely, figure 17c shows that computed head values from perturbed ground-water withdrawal values match determined head values along the boundary portions of the profile but deviate from the determined head values along the central portions of the profile. Computed head values from perturbed storage coefficient values illustrate a similar behavior as computed head values from perturbed ground-water withdrawal values (fig. 17d). Figures 17c and 17d show that doubling ground-water withdrawal values has a similar affect on computed head values as halving storage coefficient values.

Perturbed transmissivity, recharge, ground-water withdrawal and storage coefficient values exhibit the same relationships in figure 18 as in figure 17.

The sensitivity analysis shows that, when input parameters are increased, the parameters inducing the greatest cumulative error (greatest affect on computed head values) are transmissivity and ground-water withdrawal. On the other hand, when input parameters are decreased, the parameters inducing the greatest cumulative error (greatest affect on computed head values) are storage coefficient and transmissivity.

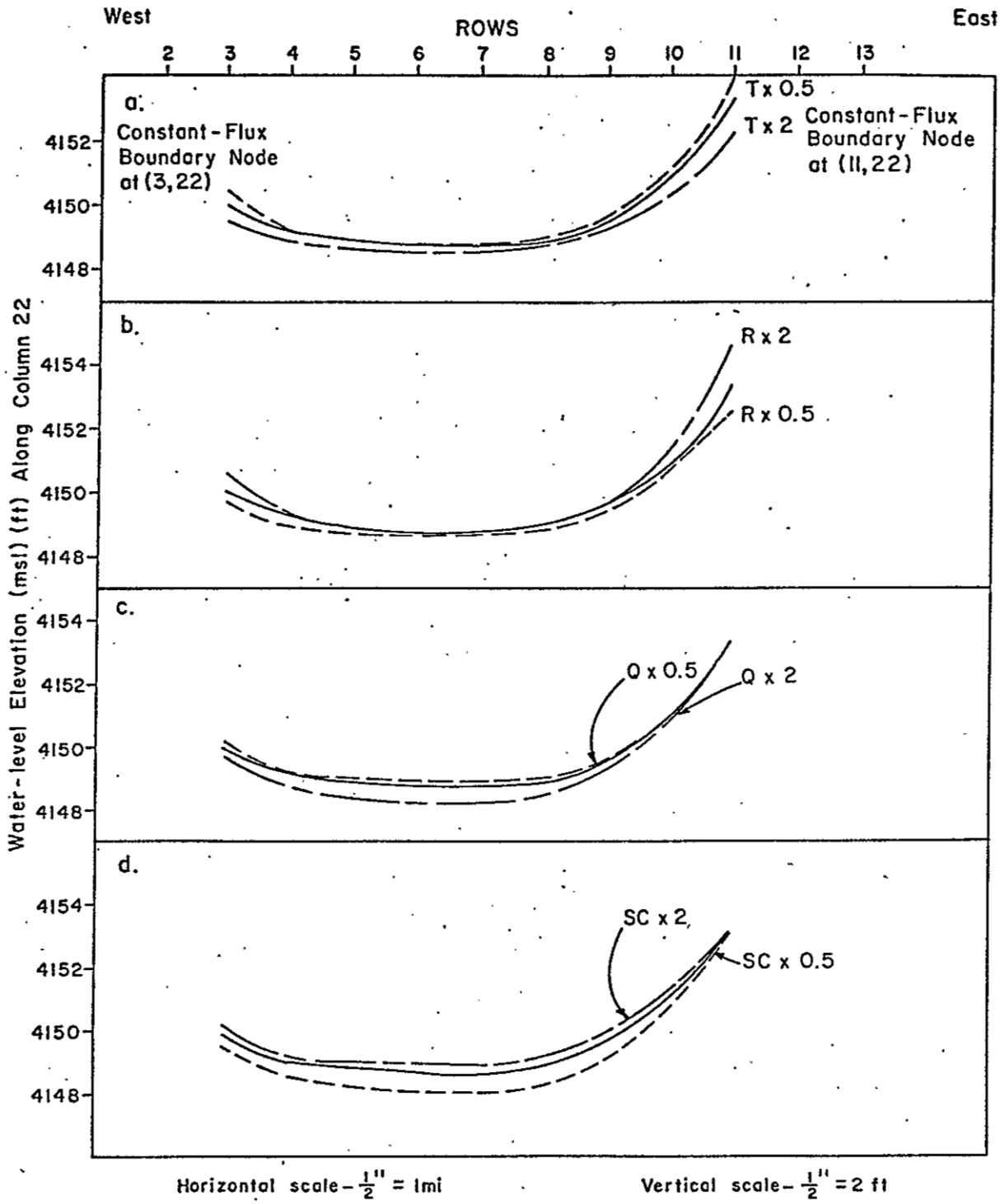

Figure 18. Model sensitivity results along column 22 (east-west profile of water levels). Transmissivity (T), mountain-front recharge (R), ground-water withdrawal (Q), and storage coefficient (SC) values are perturbed by factors of 0.5 and 2.

REFERENCES

Armstrong, A.K, Silberman, M.L., Todd, V.R., Hoggatt, W.C., and Carten, R.B., 1978, Geology of central Peloncillo Mountains, Hidalgo County, New Mexico: New Mexico Bureau of Mines and Mineral Resources, Circular 158, 19 p.

Arras, M.M.R., 1979, Geohydrological investigation in the Animas Valley, Hidalgo County, New Mexico: M.S. thesis, New Mexico State University, 84 p.

Brown, S.G., and Schumann, H.H., 1969, Geohydrology and water utilization in the Willcox basin, Graham and Cochise Counties, Arizona: U.S. Geological Survey Water Supply Paper 1859-F, p. F1-F32

Clemons, R.E., 1983, Geologic highway map of New Mexico: New Mexico Geological Society, scale 1:1,000,000

Cox, D.N., 1973, Soil Survey of Hidalgo County, New Mexico: U.S. Dept. of Agriculture, Soil Conservation Service and Forest Service, in cooperation with New Mexico Agricultural Experiment Station, 90 p.

Dane, C.H., and Bachman, G.O., 1965, Geologic map of New Mexico: U.S. Geological Survey Special Geologic Map, scale 1:500,000

Deal, E.G., Elston, W.E., Erb, E.E., Peterson, S.L., Reiter, D.E., Damon, P.E., and Shafiqullah, M., 1978, Cenozoic volcanic geology of the Basin and Range province in Hidalgo County, southwestern New Mexico: New Mexico Geological

Society Guidebook 29th field conference, p. 219-229

Doty, G.C., 196Ø, Reconnaissance of ground water in Playas Valley, Hidalgo County, New Mexico: New Mexico State Engineer, Technical Report 15, 4Ø p.

Drewes, Harald, 1982, Some general features of the El Paso-Wickenburg transect of the Cordilleran Overthrust Belt, Texas to Arizona: Rocky Mountain Association of Geologists, 1982 Field Conference Guidebook, p. 88-96

Drewes, Harald, 1972, Structural Geology of the Santa Rita Mountains, southeast of Tucson, Arizona: U.S. Geological Survey Professional Paper 748, 35 p.

Drewes, H., and Thorman, C.H., 198Ø, Geologic Map of the Steins Quadrangle and the Adjacent Part of the Vanar Quadrangle, Hidalgo County, New Mexico: U.S. Geological Survey Miscellaneous Investigations Series Map I-122Ø, scale 1:24,ØØØ

Drewes, H., and Thorman, C.H., 198Øa, Geologic Map of the Cotton City Quadrangle and the Adjacent Part of the Vanar Quadrangle, Hidalgo County, New Mexico: U.S. Geological Survey Miscellaneous Investigations Series Map I-1221, scale 1:24,ØØØ

Elston, W.E., Erb, E.E., and Deal, E.G., 1979, Tertiary geology of Hidalgo County, New Mexico: New Mexico Geology, v. 1, no. 1, p. 1-6

Flege, R.F., 1959, Geology of Lordsburg Quadrangle, Hidalgo County, New Mexico: New Mexico Bureau of Mines and Mineral Resources, Bull. 62, 36 p.

Fleischhauer, H.L., Jr., and Stone, W.J., 1982, Quaternary geology of Lake Animas, Hidalgo County, New Mexico: New Mexico Bureau of Mines and Mineral Resources, Circular 174, 25 p.

Geraghty and Miller, Incorporated, 197Ø, Ground-water report, Empire Ranch area, Pima and Santa Cruz Counties, Arizona

Gillerman, E., 1958, Geology of the Central Peloncillo Mountains, Hidalgo County, New Mexico, and Cochise County, Arizona: New Mexico Bureau of Mines and Mineral Resources, Bulletin 57, 152 p.

Hawkins, D.B., 1981, Geohydrology of the lower Animas Valley, Hidalgo County, New Mexico--A computer simulation study: M.S. thesis, New Mexico Institute of Mining and Technology, 1Ø5 p.

Hawkins, D.B., and Stephens, D.B., 1981, Hydrologic Study of the Animas Valley-Lightning Dock KGRA Areas: New Mexico Energy Institute, Final Technical Report, Fiscal Year 1981, 9Ø p.

Hayes, P.T., 1982, Geologic map of Bunk Robinson Peak and Whitmire Canyon Roadless Areas, Coronado National Forests, NM and AZ: U.S. Geological Survey Miscellaneous Field Studies Map MF-1425-A

Jacob, C.E. 1944, Notes on determining permeability by pumping tests under water-table conditions: U.S. Geological Survey, unpublished report

Jiracek, G.R., and Smith, C., 1976, Deep resistivity investigations at two KGRA's in New Mexico: Radium Springs and Lightning Dock, in Woodward, L.A. and Northrup, S.A. (eds.), Tectonics and Mineral Resources of Southwestern North America: New Mexico Geological Society Special Publication 6, p. 71-76

Kafri, U., Randall, J.H., and Simpson, E.S., 1976, Effects of ground-water pumpage on surface and ground-water flows in adjoining basins: An interim report, University of Arizona Water Resources Research Center

Kafri, U., and J. Ben-Asher, 1978, Computer estimates of natural recharge through soils in southern Arizona, U.S.A.: Journal of Hydrology, vol. 38, no. 1/2, p. 125-138

Kottlowski, F.E., Foster, R.W., and Wengerd, S.A., 1969, Key oil tests and stratigraphic sections in southwestern New Mexico: New Mexico Geological Society Guidebook, 20th Field Conference, p. 186-196

Lance, J.O., Jr., Keller, G.R., and Aiken, C.L.V., 1982, A regional geophysical study of the western overthrust belt in southwestern New Mexico, West Texas, and Northern Chihuahua: Rocky Mountain Association of Geologists, 1982 Field Conference Guidebook, p. 123-130

Lansford, R.R., Sorensen, E.F., Gollehon, N.R., Fishburn, M., Loslebon, L., Creel, B.J., West, F.G., 1980, Sources of irrigation water and irrigated and dry cropland acreages in New Mexico by county, 1974-1979: New Mexico Agricultural Experiment Station, Research Report 422, 39 p.

Lasky, S.G., 1938, Geology and ore deposits of the Lordsburg mining district, Hidalgo County, NM: U.S. Geological Survey Bulletin 885, 62 p.

Lepley, Larry, 1981, Lineament map of the State of New Mexico: New Mexico Energy Institute, Final Technical Report, Fiscal Year 1981, 21 p.

Logsdon, M.J., 1981, The aqueous geochemistry of the Lightning Dock Known Geothermal Resource Area, Animas Valley, Hidalgo County, New Mexico: M.S. thesis, University of New Mexico, 239 p.

Lohse, R.L., 1981, Temperature studies in southwestern New Mexico: New Mexico Energy Institute, Final Technical Report, Fiscal Year 1981, p. 37-82

Maker, H.J., Cox, D.N., and Anderson, J.U., 1970, Soil associations and land classification for irrigation, Hidalgo County, New Mexico: New Mexico Agricultural Experiment Station, Research Report 177, 28 p.

Morrison, R.B., 1965, Geologic map of the Duncan and Canador Peak Quadrangles, Arizona and New Mexico: U.S. Geological Survey

Miscellaneous Geologic Investigations Map I-442, scale 1:48,000

Nuzman, C., 1970, Water supply and utilization, Empire-Sonoita planning area, Pima and Santa Cruz Counties, Arizona: Layne-Western Company Incorporated

O'Brien, K.M., and Stone, W.J., 1981, Water-level data compiled for hydrogeologic study of Animas Valley, Hidalgo County, New Mexico: New Mexico Bureau of Mines and Mineral Resources Open-file Report 130, 64 p.

O'Brien, K.M., and Stone, W.J., 1982a, Water-quality data compiled for hydrogeologic study of Animas Valley, Hidalgo County, New Mexico: New Mexico Bureau of Mines and Mineral Resources Open-file Report 131, 25 p.

O'Brien, K.M., and Stone, W.J., 1982b, Drill-hole and testing data compiled for hydrogeologic study of Animas Valley, Hidalgo County, New Mexico: New Mexico Bureau of Mines and Mineral Resources Open-file Report 132, 79 p.

Reeder, H.O., 1957, Ground Water in Animas Valley, Hidalgo County, New Mexico: New Mexico State Engineer, Technical Report 11, 101 p.

Reeder, H.O., (ed.), 1959, Ground-water levels in New Mexico, 1956: New Mexico State Engineer, Technical Rept. 19, 251 p.

Reeder, H.O. (ed.), 1960, Ground-water levels in New Mexico, 1957: New Mexico State Engineer, Technical Rept. 22, 306 p.

Sanford, A.R., 1968, Gravity Survey in Central Socorro County, New Mexico: New Mexico Bureau of Mines and Mineral Resources, Circular 91, 14 p.

Schwennesen, A.T., 1918, Ground Water in the Animas, Playas, Hachita, and San Luis Basins, New Mexico: U.S. Geological Survey Water-Supply Paper 422, 152 p.

Smith, C., 1978, Geophysics, Geology and Geothermal Leasing Status of the Lightning Dock KGRA, Animas Valley, New Mexico: New Mexico Geological Society, Guidebook 29th field conference, p. 343-348

Sorenson, E.F., 1977, Water Use by categories in New Mexico counties and river basins, and irrigated and dry cropland acreage in 1975: New Mexico State Engineer, Technical Rept. 41, 34 p.

Soulè, J.M., 1972, Structural geology of Northern Part of Animas Mountains, Hidalgo County, New Mexico: New Mexico Bureau of Mines and Mineral Resources, Circular 125, 15 p.

Stone, W.J., and Mizell, N.H., 1977, Geothermal resources of New Mexico--a survey of work to date: New Mexico Bureau of Mines and Mineral Resources, Open-file Report 73, 117 p.

Stone, W.J., and Mizell, N.H., and Hawley, J.W., 1979, Availability of geological and geophysical data for the eastern half of the U.S. Geological Survey's Southwestern Alluvial Basins Regional Aquifer Study: New Mexico Bureau of

Mines and Mineral Resources, Open-file Report 109, 80 p.

Summers, W.K., 1976, Catalog of thermal waters in New Mexico: New Mexico Bureau of Mines and Mineral Resources Hydrologic Report 4, 80 p.

Summers, W.K., 1967, A comparison of long term and short term pumping tests, Ground Water, v. 5, no. 3, p. 33-34

Telford, W.M., Geldart, L.P., Sheriff, R.E., and Keys, D.A., 1976, Applied Geophysics: New York, NY, Cambridge Univeristy Press, 860 p.

Thompson, Sam, III, 1981, Analyses of petroleum source and reservoir rocks in southwestern New Mexico: New Mexico Energy Research and Development Institute, 120 p.

Thompson, Sam, III, Tovar R., J.C., and Conley, J.N., 1978, oil and gas exploration wells in the Pedregosa Basin: New Mexico Geological Society, Guidebook 29th field conference, p. 331-342

Thorman, C.H., and Drewes, H., 1978, Geolgoic Map of the Gary and Lordsburg Quadrangles, Hidalgo County, New Mexico: U.S. Geological Survey Miscellaneous Investigation Series Map I-1151, scale 1:24,000

Trauger, F.D., 1972, Water resources and general geology of Grant County, New Mexico: New Mexico Bureau of Mines and Mineral Resources, Hydrologic Report 2, 211 p.

Trescott, P.C., Pinder, G.F., and Larson, S.P., 1976, Finite-

difference model for aquifer simulation in two dimensions with results of numerical experiments: U.S. Geological Survey Techniques of Water-Resources Investigations, Chapter C1, Book 7, 116 p.

White, N.D., and Hardt W.F., 1965, Electrical-analog analysis of hydrologic data for San Simon basin, Cochise and Graham Counties, Arizona: U.S. Geological Survey Water Supply Paper 1809-R, p. R1-R30

Walton, W.C., 1970, Groundwater Resource Evaluation: New York, McGraw-Hill, Inc., 664 p.

Wilson, L.G., DeCook, K.J., and Newman, S.P., 1980, Regional recharge research for southwest alluvial basins: Water Resources Research Center, Tucson, Arizona

Wynn, J.C., 1981, Complete Bouguer anomaly map of the Silver City $1^{o}x2^{o}$ quadrangle, New Mexico-Arizona: U.S. Geological Survey Miscellaneous Investigation Series Map I-1310-A

Wrucke, C.T., and Bromfield, C.S., 1961, U.S. Geological Survey Mineral Investigation Field Studies Map MF-160

Zeller, R.A., Jr., 1962, Reconnaissance geologic map of Southern Animas Mountains, New Mexico Bureau Mines and Mineral Resources Geologic Map 17, scale 1:62,500